Helsinki Eye Lab
Department of Ophthalmology
Faculty of Medicine
University of Helsinki
Finland

TEAR FILM LIPID LAYER – FROM COMPOSITION TO FUNCTION

IMPLICATIONS OF THE ANTI-EVAPORATIVE EFFECT

Antti H. Rantamäki

ACADEMIC DISSERTATION

To be presented for public examination with the permission of the Faculty of Medicine, University of Helsinki, in Auditorium Christian Sibelius, Välskärinkatu 12, Helsinki, on February 7th 2014, at 12 noon.

Helsinki 2014

Supervisors

Adjunct Professor Juha Holopainen
Helsinki Eye Lab
Department of Ophthalmology
University of Helsinki
Helsinki, Finland

and

Adjunct Professor Susanne Wiedmer
Department of Chemistry
University of Helsinki
Helsinki, Finland

Reviewers

Professor Ben Glasgow
The Jules Stein Eye Institute
David Geffen School of Medicine
University of California
Los Angeles, California, USA

and

Professor J. Peter Slotte
Laboratory of Lipid and Membrane Biochemistry
Department of Biosciences
Åbo Akademi University
Turku, Finland

Opponent

Professor Emeritus Anthony J. Bron
Nuffield Laboratory of Ophthalmology
Nuffield Department of Clinical Neurosciences
University of Oxford
Oxford, United Kingdom

ISBN 978-952-10-9726-3 (Paperback)
ISBN 978-952-10-9727-0 (PDF, http://ethesis.helsinki.fi)
Unigrafia 2014

Don’t despair; the situation is no worse than most things in science.

TABLE OF CONTENTS

LIST OF ORIGINAL PUBLICATIONS

This thesis is based on the following original publications, which will be referred to in the text by their Roman numerals:

I. Antti H. Rantamäki, Tuulikki Seppänen-Laakso, Matej Oresic, Matti Jauhiainen, Juha M. Holopainen 2011. Human tear fluid lipidome: from composition to function. *PLoS ONE 6*: e19553

II. Antti H. Rantamäki, Matti Javanainen, Ilpo Vattulainen, Juha M. Holopainen 2012. Do lipids retard the evaporation of the tear fluid? *Invest. Ophthalmol. Vis. Sci. 53*: 6442-6447

III. Antti H. Rantamäki, Susanne K. Wiedmer, Juha M. Holopainen 2013. Melting points – The key to the anti-evaporative effect of the tear film wax esters. *Invest. Ophthalmol. Vis. Sci. 54*: 5211–5217

ABBREVIATIONS

ADDE	aqueous-deficient dry eye
AO	arachidyl oleate
BAl	behenyl alcohol
BAM	Brewster angle microscope/microscopy
BL	behenyl laurate
BLN	behenyl linoleate
BLNN	behenyl linolenate
BO	behenyl oleate
BP	behenyl palmitoleate
CE	cholesteryl ester
CO	cholesteryl oleate
DPPC	dipalmitoyl phosphatidylcholine
EDE	evaporative dry eye
eggPC	egg-yolk L-alpha phosphatidylcholine
LC	liquid-condensed (phase)
LE	liquid-expanded (phase)
LL	lignoceryl lignocerate
LO	lauryl oleate
MP	melting point
MS	mass spectrometer/spectrometry
OAHFA	(O-acyl)-omega-hydroxy fatty acid
PBS	phosphate buffered saline
PC	phosphatidylcholine
PE	phosphatidylethanolamine
PL	phospholipid
PLTP	phospholipid transfer protein
PS	phosphatidylserine
Q-TOF-MS	quadrupole time-of-flight mass spectrometer
SM	sphingomyelin
SP	surfactant protein
TG	triglyceride
TLC	thin layer chromatography
UPLC	ultra performance liquid chromatography
WE	wax ester

ABSTRACT

The tear film lining the ocular surface consists of three qualitatively different layers. The hydrated (*i*) mucous matrix, which is composed of the epithelial glycocalyx and secreted gel-like mucins, continues as a concentration gradient into the overlaying protein-rich (*ii*) aqueous layer, which is largely responsible for the hydration, nutrition, and host defence of the ocular surface. Finally, the air-tear interface is lined with a thin (*iii*) tear film lipid layer (TFLL), which is considered to stabilise the entire tear film and is thought to retard evaporation from the air-tear interface. Meibum, an oily secretion produced by meibomian glands, is considered largely as the source of the TFLL lipids. The integrity of the tear film is vital for the ocular surface, and disturbances in any of the aforementioned sections typically result in dry eye symptoms. Despite the extremely low evaporation rates measured from the ocular surface *in vivo*, no evaporation-retarding mechanism of TFLL has been shown *in vitro*. Altogether, due to the co-operative character of lipids, the function and behaviour of the TFLL and similar lipid layers are largely defined by their lipid composition. To understand the behaviour of complex lipid layers on the molecular level, the composition of the layer should be determined. Therefore, the first aim of this study was to analyse the lipid composition of tear fluid. Because most of the lipids are considered to be located in the TFLL, the aim was to create TFLL-like lipid compositions for *in vitro* experiments. Finally, the aim was to investigate the evaporation-retarding effect of such lipid layers to better understand the potential mechanism of evaporation retardant *in vivo* TFLL.

A modern mass-spectrometric platform, namely ultra performance liquid chromatography coupled to quadrupole time-of-flight mass spectrometry, was employed for the tear fluid lipid analysis. In contrast to the widely recognised meibum lipid composition, the tear fluid samples contained a considerable amount of phospholipids. Unfortunately, most of the non-polar lipids, such as the cholesteryl esters and the wax esters typically present in meibum, could not be detected using this mass spectrometric platform; however, they were detected with enzymatic assays and thin layer chromatography. In addition, we demonstrated that the phospholipids function as a spreading aid facilitating the uniform spreading of the hydrophobic non-polar lipids at the air-water interface.

Based on the tear fluid lipid composition, we created TFLL-like lipid compositions and investigated their ability to retard evaporation from the air-water interface *in vitro*. A custom-built system was assembled for evaporation rate determination, and Brewster angle microscopy was employed to observe the interfacial organisation of the lipid layer at the air-water interface. It was found that very specific lipids and very definite lipid compositions are needed to retard evaporation from the air-water interface. None of the complex TFLL-like lipid compositions retarded evaporation. However, a specific class of TFLL lipids, namely wax esters (WEs), were shown to be efficient evaporation retardants, but layers composed of WEs mixed with large proportions of other TFLL lipids did not retard evaporation.

WEs, however, did not retard evaporation under all conditions, but only in a defined phase of the layer. This phase and therefore the evaporation-retarding effect was dependent on the melting point of the specific WE and the temperature of the air-water

interface. The WEs that were close to their bulk melting temperature retarded evaporation, whereas the WEs in their solid or liquid states lacked this property. In their solid state, the WEs did not spread as a uniform layer at the air-water interface, whereas in their liquid state, the WEs formed very fluid layers, and therefore, the water molecules diffused through the loosely packed lipid layer. We also investigated the surface-active properties of WEs and noted that WEs are expectedly poor surfactants compared to phospholipids; they are extremely prone to aggregation and are poorly compressible, especially when the layer is in the evaporation-retarding phase. These results support the theory suggested in our lipid composition study: hydrophobic lipids need to be mixed with a certain amount of amphiphilic lipids to form rapidly spreading films at the air-water interface.

In summary, this thesis project concentrated on providing an *in vitro* model for linking certain functions, properties, and behaviours of TFLL to the composition of such layers. In short, amphiphilic phospholipids seem to be a vital component of the TFLL, although possibly in a smaller proportion than originally hypothesised, providing aid for non-polar lipid spreading. The evaporation-retarding effect is largely dependent on the composition. Pure WEs turned out to be effective evaporation-retarding TFLL lipids, but only in a certain temperature-dependent phase. Therefore, WEs are most likely the lipids that provide the evaporation-retarding effect of the TFLL; however, such complex evaporation-retarding lipid composition is yet to be determined *in vitro*. The results of this thesis suggest that the compositional changes affect the behaviour, such as spreading and the evaporation-retarding effect, of TFLL. Defects in such properties may result in accelerated evaporation from the ocular surface and, consequently, in dry eye symptoms.

1. INTRODUCTION

The tear film is a few-micron-thick aqueous film lining the ocular surface epithelium (Whikehart 2004). It performs a number of functions, including protection of the ocular surface and providing nutrition for the cornea. Being the protective interface between the surrounding environment and the epithelium, the integrity of the film is essential for the health of the cornea and the ocular surface. The tear film is affected by destabilising factors such as gravity, capillary forces induced by the menisci of the lids, and the surface tension of the aqueous interface that induces curvature of the interface and therefore dewetting of the ocular surface (Wong et al. 1996, Miller et al. 2002, Braun and Fitt 2003). Additionally, evaporation of the aqueous tear is a considerable factor that affects the tear film integrity (King-Smith et al. 2009).

An oily film, with a thickness in the range of tens to hundreds of nanometres (King-Smith et al. 2010), lines the air-tear interface of the tear film. The function of this tear film lipid layer (TFLL) is to diminish the effect of the aforementioned destabilising factors. This function is thought to occur mainly through a decrease in surface tension and possibly by viscoelastic properties of the TFLL, providing physical support for the entire tear film (Wong et al. 1996, Rosenfeld et al. 2013). Importantly, it is also believed that the TFLL is an effective evaporation retardant, forming a physical barrier that partly retards diffusion (mass transfer) of water molecules from the air-tear interface. Therefore, the disturbances in the tear film lipid secretion may result in a less efficient barrier and consequently faster evaporation from the interface and possible dry eye symptoms (Lemp et al. 2007).

The underlying mechanism of the retardation of evaporation by TFLL is not established, which is partly because the composition of the TFLL is not entirely known. A considerable portion of the lipids originates from meibum, an oily secretion produced by meibomian glands (Butovich et al. 2008). Meibum has been shown to mainly contain very hydrophobic lipids, which are prone to aggregation at the air-water interface. However, the composition of meibum differs from that of TFLL. Researchers have mainly debated the concentration of polar phospholipids (PLs) in TFLL (Butovich 2013). In meibum, the proportion of PLs is very low compared to the non-polar lipids, but in tear fluid, the phospholipids are thought to be more abundant. It has been suggested that the polar lipids, if present in TFLL, would facilitate the uniform spreading of the lipids at the air-water interface and that the multi-layered structure formed by the polar and non-polar lipids would effectively retard evaporation (McCulley and Shine 1997).

Therefore, in this thesis project, we have investigated the lipid composition of the tear fluid. Specifically, we concentrated on the PL composition of the tear fluid and attempted to illustrate the possible effect of PLs in TFLL. Secondly, based on the tear fluid lipid composition, we studied the evaporation-retarding effect of the TFLL-like lipid layers *in vitro*. An additional aim was to investigate which physicochemical properties of the lipid layer result in an evaporation-retardant layer. Finally, we investigated the evaporation-retarding effect and the surface-active properties of a specific TFLL-lipid class, namely wax esters (WEs).

2. REVIEW OF THE LITERATURE

2.1 Corneal anatomy

The cornea is an avascular and transparent layered tissue located in the anterior region of the eye. It forms approximately 45 D of the 60-70 D total refractive power of the eye. The central and peripheral thicknesses of the cornea range from 500 to 550 μm and from 600 to 700 μm, respectively (Doughty and Zaman 2000, Ehlers and Hjortdal 2004, Salvetat et al. 2011). This difference in thickness results in an aspherical curvature of the cornea. Frontally viewed, the cornea has an elliptical shape with a horizontal average diameter of 12 mm (Rufer et al. 2005).

2.1.1 Corneal structure

The cornea consists of epithelium, Bowman's layer, stroma, Descemet's membrane, and endothelium. It is built around a collagen sheet structure, which provides mechanical strength but is also transparent and therefore allows undisturbed access of light into the eye (Figure 1).

The epithelium is the anterior layer of the cornea with a thickness of 50 μm (Ehlers 1970). It contains five to six layers of non-keratinised squamous stratified epithelial cells, which are divided into three morphological classes. (*i*) The apical cells consist of two to three layers of flat-shaped cells joined via desmosomes and tight junctions (Hsu et al. 1999, Ban et al. 2003). The junctions form a seal between the neighbouring cells that prevents the leakage of the tear fluid and impurities from the tear film into the stroma. The apical face of these superficial cells is covered with microvilli and microplicae, which increase the contact surface area between the epithelium and the tear film and therefore promote the absorption of metabolites and oxygen from the tear fluid (Nichols et al. 1983). The apical surface is also lined with transmembrane glycoproteins and mucins. This epithelial glycocalyx interacts with the tear fluid mucins, forming a network-like mucous matrix across the tear film (Spurr-Michaud et al. 2007, Mantelli and Argueso 2008). (*ii*) The wing cells, an intermediate epithelial cell type, form a layer of two to three cells between the apical and basal cells. (*iii*) The basal cells form a single layer of cells between the wing cells and the underlying basement membrane. The basement membrane, secreted by the basal cells, is an extracellular matrix, which functions in anchoring, migration and maintenance of the associated cells (Torricelli et al. 2013). The basal cells are connected to the basement membrane via hemidesmosomes and further to Bowman's layer via basement-layer-penetrating fibrils (Gipson et al. 1987).

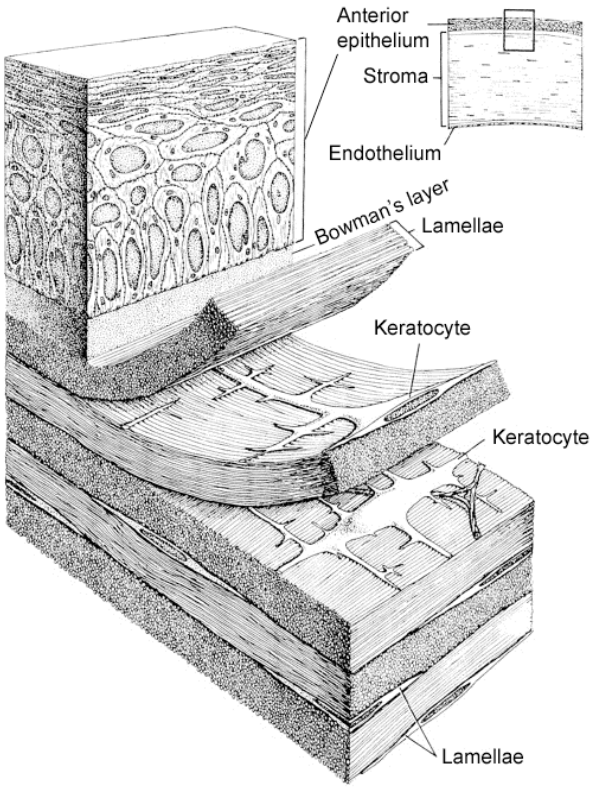

Figure 1. Cross-sectional diagram illustrating the anterior section of the cornea: epithelium, Bowman's layer, stromal lamellae, and keratocytes. Adapted from Ehlers and Hjortdal 2006.

The epithelium completely regenerates over a period of seven to ten days (Hanna et al. 1961, Cenedella and Fleschner 1990, Ehlers and Hjortdal 2006). The stem cells located in the limbal areas of the cornea continuously produce new basal cells, which migrate towards the centre of the cornea and further differentiate into wing cells and finally to apical cells. At the end of their life cycle, the apical cells desquamate from the epithelium after involution and apoptosis, and the flow of tear fluid drains the cell residues from the ocular surface.

Bowman's layer is a non-regenerative, 8-12 μm thick acellular layer of proteoglycans (Komai and Ushiki 1991) and collagens (type I, III, V, and VI) that separates the epithelium and the stroma (Marshall et al. 1993). This dense meshwork-like layer enhances the adhesion between the epithelium and the stroma through the basal cell collagen VII fibrils and the collagen IV anchoring plaques (Gipson et al. 1987).

The corneal stroma comprises approximately 90% of the overall corneal thickness, and it mainly consists of type I, type III, and type V fibril-forming and type VI beaded filament-forming collagen bundled into the lamellar structures (Ihanamaki et al. 2004, Whikehart 2004). The longitudinally running fibres in adjacent lamella lie at different angles to each other, providing the mechanical strength for the cornea.

Keratocytes, the quiescent stromal fibroblasts, are the main cell population in the stroma (West-Mays and Dwivedi 2006). The cells are arranged in a corkscrew-like fashion between the lamellae to attain a uniform distribution in the stroma (Müller et al.

1995). Keratocytes are responsible for maintaining the stromal structure and in particular for repairing the tissue after stromal injuries (Jester et al. 1999, Fini and Stramer 2005, West-Mays and Dwivedi 2006).

Descemet's membrane, a basement membrane secreted by the underlying endothelium, is a layer of collagens IV, VI, and VII that forms a dense flexible network accompanied by laminins and fibronectin (Marshall et al. 1993, Beuerman and Pedroza 1996). Like Bowman's layer, the Descemet's membrane does not regenerate, but it does increase its thickness with age.

The endothelium, formed by a single layer of cells, forms the interior layer of the cornea (Waring et al. 1982). The main functions of the endothelium are to supply the diffusion of metabolites and nutrients for the stromal and epithelial cells and to maintain the hydration level and, therefore, the transparency of the corneal stroma. The balance across this leaky barrier is maintained by the ionic pumps located in the endothelial cell plasma membranes.

2.1.2 Corneal innervation

The human cornea is a densely innervated tissue. Most of the corneal nerve fibres are the sensory type, and they originate from the ophthalmic division of the trigeminal nerve (Zander and Weddel 1951, Rozsa and Beuerman 1982). The inferior corneal innervation may also originate from the trigeminal maxillary branch (Vonderahe 1928, Ruskell 1974). In addition, the cornea receives sympathetic innervation from superior cervical ganglion; however, the fibre density seems to differ between mammalian species (Marfurt and Ellis 1993). In addition, parasympathetic innervation has been reported in certain mammalian corneas, such as rats and cats (Tervo et al. 1979, Morgan et al. 1987, Marfurt et al. 1998)

The nerve fascicles (bundles) enter the cornea radially and protrude into the peripheral areas of the stroma parallel to the collagen fibres (Müller et al. 2003). Close to the limbal area of the cornea, the nerve bundles and fibres divest of their perineurium and myelin sheaths, respectively, to maintain the transparency of the cornea. The bundles protrude towards the central area of the cornea surrounded by the Schwann cell sheaths. The bundles divide into separate branches and bend 90 degrees, penetrating Bowman's layer. The bundled fibres divest of the Schwann sheaths (Müller et al. 1996) and make another abrupt 90 degree bend and form a sub-basal nerve plexus between Bowman's layer and the basal cells (Müller et al. 1997). From the sub-basal nerve plexus, individual fibres separate and course towards the epithelial cells and finally terminate between the superficial layers of the epithelium.

2.2 Dry eye syndrome

Dry eye is a multifactorial disease of the ocular surface that results in symptoms of discomfort and visual disturbance (Lemp et al. 2007). It is accompanied by elevated osmolarity of the tear film and ocular surface inflammation with potential damage to the ocular surface. Typical symptoms are dryness, redness, foreign body sensation, itching, and burning of the eyes. Combined data from population-based studies show that the prevalence of dry eye ranges from 5% to 30% in over 50-year-olds, which makes dry eye syndrome the most common ocular problem (Smith et al. 2007).

Based on the most recent classification, dry eye syndrome is divided into two major classes, aqueous-deficient dry eye (ADDE) and evaporative dry eye (EDE). In ADDE, the symptoms arise from a failure in lacrimal tear secretion. Dry eye induced by lacrimal acinar destruction or dysfunction results from reduced tear secretion and volume (Mishima et al. 1966, Scherz and Dohlman 1975). Due to the protracted secretion of aqueous tears, the evaporation of the water from the ocular surface renders the tear fluid hyperosmolar. These hyperosmolar conditions stimulate a cascade of inflammatory events in the epithelial cells. ADDE may have several causes, such as Sjögren Syndrome (Lemp et al. 2007), aging (Mathers et al. 1996), inflammatory infiltration of the lacrimal glands (James et al. 1964, Heath 1948) or sensory reflex block of the corneal nerves (Heigle and Pflugfelder 1996, Battat et al. 2001).

In EDE, both intrinsic and extrinsic causes result in excess evaporation of the tear fluid. Intrinsic causes are due to intrinsic disease affecting lid structure or dynamics, whereas extrinsic causes are due to an external factor. However, the boundary between these two causes is blurred. The most common reason for EDE is meibomian gland dysfunction, a condition caused by obstruction of the meibomian glands that often leads to posterior blepharitis (Foulks and Bron 2003, Bron et al. 2004, Bron and Tiffany 2004). Meibomian gland dysfunction is associated with dermatoses, such as acne rosacea, seborrhoeic dermatitis (McCulley and Dougherty 1985), and atopic dermatitis. Other intrinsic causes may be disorders of the lid aperture caused by exposure of the ocular surface, and therefore, increase in evaporative surface area, in craniostenosis, proptosis, and high myopia (Gilbard and Farris 1983, Lemp et al. 2007). Additionally, low blink rate during activities involving intensive gazing, such as working at video screens, causes increased evaporation from the exposed ocular surface (Nakamori et al. 1997). Low blink rate is also associated with neurological disorders, such as Parkinson Disease (Karson et al. 1984). Typical extrinsic causes include ocular surface disorders, such as xerophthalmia due to vitamin A deficiency (Tei et al. 2000), epithelial cell damage due to eye drop preservative benzalkonium chloride (Uusitalo et al. 2010), contact lens wear (Schlanger 1993, Pritchard and Fonn 1995), and allergic conjunctivitis (Lemp et al. 2007).

The causative mechanism of dry eye syndrome can be divided into two factors: tear hyperosmolarity and tear film instability (Lemp et al. 2007). Hyperosmolarity is considered the key mechanism that causes inflammation, damage, and symptoms on the ocular surface and promotes the compensatory events of dry eye, such as reflex stimulation of the lacrimal gland. A hyperosmolar state may arise due to inadequate tear production (and normal rate of evaporation), due to excessive evaporation from the

ocular surface or due to a combination of these two. Unstable tear film is typically caused by a premature break-up of the tear film, which results in local drying, hyperosmolarity of the exposed ocular surface, epithelial damage, and disturbances of the glycocalyx and the mucous matrix.

2.3 Composition, structure, and function of the tear film

Tear fluid forms an approximately 4-11-µm film over the ocular surface (King-Smith et al. 2004). The purpose of this thin film is to protect the epithelium physically and chemically. Tear film acts as a lubricant for the lid and ocular surface interface, provides antibacterial protection, flushes contaminants from the ocular surface, acts as a nutrient for the corneal epithelium, and provides a smooth interface for the light to enter the eye (Tiffany 1997, Whikehart 2004). It consists of three qualitatively different interlacing layers that are in intimate interaction with each other (Figure 2): an interior mucin-enriched mucous matrix, a middle aqueous layer, and an anterior TFLL.

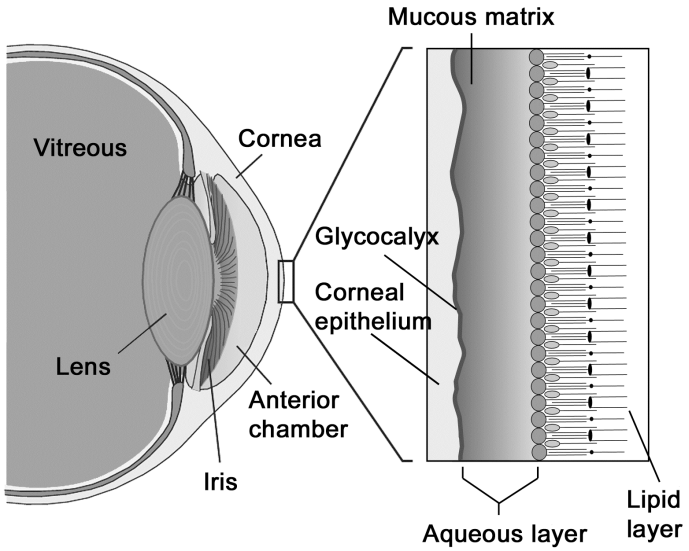

Figure 2. Cross-sectional view illustrating the layered structure of the tear film lipid layer. The dimensions are not to scale. Adapted from Rantamäki et al. 2011.

2.3.1 The mucous matrix

Mucous matrix consists of mucins, which are water-retaining, high-molecular-weight glycoproteins essential for the homeostasis of the ocular surface (Mantelli and Argueso 2008). On the ocular surface and in tear fluid, there are two groups of mucins: transmembrane, mainly MUC1, MUC4, and MUC16, and secreted gel-forming, such as abundant MUCA5C. Epithelial cells of both cornea and conjunctiva produce MUC1 (Inatomi et al. 1995) and MUC16 (Argueso et al. 2003), but only conjunctival epithelial

cells and possibly limbal corneal epithelial cells produce MUC4 (Inatomi et al. 1996). The goblet cells placed in conjunctiva secrete the gel-forming mucins.

The transmembrane mucins form part of the corneal and conjunctival glycocalyx, and the gel-forming mucins interact with this hydrophilic glycocalyx to form a loose network-like matrix (Tiffany 1997). The mucous matrix does not have a precisely defined structure but continues as a concentration gradient throughout the aqueous phase.

The mucous matrix is thought to increase the hydrophilic character of the epithelium, thereby enhancing the wetting properties of the ocular surface. For instance, the tear film does not spread as a uniform layer in the area of a corneal ulcer (Watanabe 2002). The scarred epithelium lacks transmembrane mucins, while the goblet cells still secrete gel-forming mucins. This suggests that the transmembrane mucins in particular are crucial for the wetting of the epithelium and that gel-forming mucins alone are not able to form a wettable surface because they lack a suitable interface for interaction. In addition, the mucous matrix is also very vulnerable to certain exogenous chemicals, such as benzalkonium chloride, which is typically used as a preservative for certain topical ophthalmic solutions. This vulnerability is due to the toxicity of benzalkonium chloride to the epithelial cells, specifically to goblet cells producing gel-forming mucins (Uusitalo et al. 2010). Therefore, benzalkonium-chloride-induced defects in the mucous matrix may hinder wetting of the ocular surface.

The mucous network and the high molecular weight of the mucins may give tear fluid its viscous appearance and may increase the stability of the tear film. However, this function is somewhat questionable due to the low concentration (<300 μg/mL) of tear fluid mucins (Bron et al. 2004). The mucous-network may also be responsible for preventing adhesion of the pathogens to the ocular surface (Kardon et al. 1999, Blalock et al. 2007).

2.3.2 The aqueous layer

The aqueous layer contains electrolytes, proteins, and metabolites. The aqueous tears and part of the solutes are produced in the lacrimal system, the lacrimal gland, and the accessory lacrimal glands. In addition, the ocular surface epithelial cells have a contribution to the protein composition. Tear fluid is rich in protein; the typical concentration is 7-10 mg/mL (Whikehart 2004, Tiffany 1997). As many as ~500 proteins have been identified in tear fluid (de Souza et al. 2006). Many of the proteins are involved in wound healing, inflammatory processes, and protection of the cornea from various pathogens. Tear fluid proteins may also interact with the lipid layer, and thus, they may have a biophysical function in the stabilisation and organisation of the TFLL.

The most abundant proteins in the tear fluid are lysozyme, lactoferrin, tear lipocalin (tear-specific prealbumin), secretory immunoglobulin A, lipophilin, immunoglobulin G, and serum albumin (Tiffany 1997). Lysozyme, or N-acetylmuramide glycanhydrolase, catalyses the hydrolysis of beta-(1-4) glycosidic linkages between bacterial cell wall carbohydrates and thereby acts as an antibacterial agent (Fleming 1922, Phillips 1967). Lactoferrin (or lactotransferrin) also exhibits antibacterial activity as a regulator of iron homeostasis (Arnold et al. 1977). It prevents harmful iron-promoted microbial growth

and free-radical-induced cellular damage (Ward et al. 2005). Lactoferrin also has antiviral and antifungal properties (Farnaud and Evans 2003). Lipophilins interact with lipids, but the specific function of tear lipophilin remains unclear (Lehrer et al. 1998).

Proteins in the tear film (despite being discussed here in the context of the aqueous layer) may also interact with both the mucous matrix and the lipids in the TFLL or may be a part of the TFLL structure. For instance, tear lipocalins bind fatty acids, fatty alcohols, PLs, glycolipids, and cholesterol (Glasgow et al. 1995), of which many are present in the TFLL. Tear lipocalin plays a role as an effective lipid-scavenger in tear fluid, transporting contaminating lipids from the corneal surface possibly to the anterior lipid layer (Glasgow et al. 1999, Glasgow et al. 2010, Gasymov et al. 2005, Yeh et al. 2013). This function is important because lipid-contaminated corneal surface exhibits impaired wetting, consequently resulting in an unstable tear film. Lipocalin also lowers the surface tension of the air-water interface and is therefore able to protrude into the lipid layer (Glasgow et al. 1999, Saaren-Seppälä et al. 2005). However, lipocalin does not show any bind-and-release activity needed for the lipid transfer, as does another lipid binding tear fluid protein – phospholipid transfer protein (PLTP) (Jauhiainen et al. 2005). Tear fluid contains twice the amount of PLTP as that in blood, but its function in the tear fluid is not precisely known. PLTP knock-out mice, however, are very prone to dry eye syndrome (Setälä et al. 2011). PLTP may be responsible for fine-tuning the lipid transport machinery of the tear fluid similar to lipocalin.

Tear film also contains other potential lipid-interacting lipids, such as group II phospholipase A2, a hydrolytic antibacterial enzyme that degrades the cell walls of gram-positive bacteria and therefore is involved in the host defence mechanism of the ocular surface (Nevalainen et al. 1994). Additionally, tear fluid contains lipid-modifying enzymes, such as acidic and neutral sphingomyelinases, acidic and neutral ceramidases, and PC-specific phospholipase C secreted by the epithelial cells (Robciuc et al. 2014). Altogether, it appears that protein-lipid interactions have a vital function in maintaining the lipid homeostasis of the tear film.

2.3.3 Tear film lipid layer (TFLL)

Lipids form a thin oily layer, a tear film lipid layer, over the aqueous tears. The lipids forming this layer are partly secreted by the meibomian glands (Butovich et al. 2008). Over the past decades, the opinion on the meibum composition has varied with the development of more advanced analysis techniques. Despite the variety of compositions, sterol esters, and WEs have retained their position as the most abundant lipid species in meibum. With increased knowledge of lipid composition and their behaviour at the air-water interface, it has become increasingly evident that the somewhat non-polar meibomian lipids need to be accompanied by polar lipids, such as PLs (McCulley and Shine 1997). The non-polar lipids cannot form a uniformly spread layer at the air-tear interface due to their physico-chemical properties, i.e., their hydrophobic nature drives them into aggregates, thus minimising the contact area with the polar water molecules (Figure 3A). However, the amphiphilic molecules, such as PLs, facilitate the spreading of the non-polar lipid species. This is attained by the formation of a layered structure, where

the PLs adopt an orientation in which their head groups are located in the water and their non-polar hydrocarbon chains point towards the air. The non-polar lipid species form an overlaying lipid layer on top of the interfacial PLs (Figure 3B). Therefore, the PL-layer effectively minimises the energetically unfavourable contact between non-polar lipids and water. This layered model is in line with tear lipocalin binding studies, which show that lipocalin readily binds amphiphilic lipids in TFLL but does not bind cholesteryl esters (CE) (Glasgow et al. 1995). This suggests that the polar lipids located at the air-tear interface hinder the interaction of lipocalin and cholesteryl esters at the overlaying non-polar layer. The source of PLs in tear fluid is still obscure; in addition to the meibomian gland, polar lipids may originate from the corneal or conjunctival epithelial cells (Butovich 2008).

One of the TFLL functions is to stabilise the tear film by lowering the aqueous tear surface tension. Tear film is also thought to retard the evaporation of water from the ocular surface. The *in vivo* studies support this theory by showing extremely low evaporation rates (Mishima and Maurice 1961, Iwata et al. 1969, Craig and Tomlinson 1997, Craig et al. 2000), whereas the few existing *in vitro* studies have not been able to show any support for this theory (Borchman et al. 2009, Herok et al. 2009, Cerretani et al. 2013).

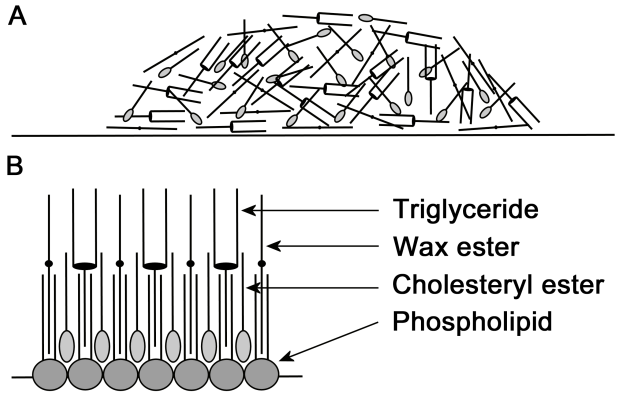

Figure 3. Hypothetical illustration of the effect of amphiphiles on the spreading of non-polar lipids. (A) Hydrophobic lipids at the air-water interface possess a tendency to aggregate and therefore do not form a homogenous lipid layer.
(B) Amphipathic phospholipids form uniform monolayers, thereby rendering the interface hydrophobic and providing a suitable interface for non-polar lipid spreading. Adapted from Rantamäki et al. 2011.

2.3.3.1 Non-polar lipids

The composition of the TFLL has become better known during the past decade, especially with the rapid development of mass spectrometric techniques. The typical study subject has been meibum due to its better availability than that of tears. Meibum primarily contains WEs and CEs. WEs cover 30-50% (Butovich et al. 2012) and CEs cover 30% (Butovich 2010) of the total meibomian lipid. The WEs are mainly unsaturated (82%); approximately 90% of the unsaturated WEs are oleates (18:1) and <10% are palmitoleates (16:1). Among the unsaturated WEs, <3% are polyunsaturated. Among the remaining 18% of saturated WEs, the acyl chain lengths range from C16 to C18, which are mostly branched. The main WE alkoxy chain lengths range from 24:0 to 27:0, and the chains are mostly branched (Nicolaides et al. 1981, Butovich 2011).

The acyl chain lengths in meibum CEs are largely longer than those encountered elsewhere in humans and animals (Butovich 2010). The chain lengths range from 16 to 32 carbons, and the major proportion consists of 26:0, 25:0, 24:0, 27:0, 24:1, 18:1, 20:0 chains.

A WE-like lipid class, (O-acyl)-omega-hydroxy fatty acids (OAHFA), originally described in meibum nearly 30 years ago (Nicolaides and Santos 1985), constitute 4% of meibum and therefore are supposedly present in the tear film lipid layer (Butovich 2013). However, until now, no studies have investigated the OAHFA content of tear fluid. OAHFAs have been reported to be significantly more hydrophilic in physiological pH than the WEs having very similar structures (Butovich 2011). This is due to the additional carboxyl group compared to WEs. Therefore, it has been suggested that the OAHFAs would be the major polar lipid in the TFLL instead of PLs. However, the surface-active behaviour of the OAHFAs at the air-water interface does not seem to differ considerably from that of WEs; both lipids show a tendency to aggregate (Schuett and Millar 2013).

In addition to the aforementioned main lipid classes, meibum also contains minor lipid species, such as triacyl glycerols, diacyl glycerol, free fatty acids (Butovich 2011), and free cholesterol (Arciniega et al. 2013).

2.3.3.2 Polar lipids

Only a few studies have recently been published regarding the lipid composition of tear fluid samples collected from the ocular surface (Ham et al. 2005, Saville et al. 2010, Saville et al. 2011, Dean and Glasgow 2012, Arciniega et al. 2013). The reasons for this are evident. The lipids in the aqueous tear samples are extremely diluted compared to the meibum, which, in contrast, is essentially pure lipid. Collecting analysable volumes of tear fluid is laborious, and the samples may become contaminated more easily during collection and handling. In addition, the employed techniques need to be highly sensitive and selective due to the low lipid concentrations. The tear fluid lipid composition seems to differ from the meibum composition and should therefore be studied in more detail.

The recent tear fluid studies have concentrated mainly on the PL content of the tear fluid. These studies have been criticised because, in such low concentrations (on the scale of micromols per litre), the PLs could not have any considerable impact on the

TFLL structure (Butovich 2013). However, these conclusions are based on rough estimations of the lipid class proportions in TFLL. The exact lipid composition of TFLL is not known because comprehensive profiling of polar and non-polar lipids cannot be performed within the same mass spectrometric method. Therefore, a reliable comparison between the polar and non-polar lipid proportions cannot be made.

Based on the very few mass spectrometric tear fluid studies, phosphatidylcholines (PCs) are the most abundant PLs in tear fluid, followed by sphingomyelin (SM) and phosphatidylethanolamine (PE) (Ham et al. 2005, Saville et al. 2010, Saville et al. 2011, Dean and Glasgow 2012). The total number of carbons in the acyl chains, both saturated and unsaturated, ranged from 30 to 40 carbons, which suggests individual chain lengths from C16 to C24. PLs have also been detected in meibum utilising mass spectrometric techniques (Saville et al. 2011, Chen et al. 2010, Lam et al. 2011, Butovich et al. 2007, Butovich et al. 2007, Butovich 2009), but in these studies, the reported proportions have been miniscule compared to the quantities of the major meibum lipids.

2.4 Tear film dynamics, blinking, and tear break-up

The quasi-stagnant tear film is in fact a somewhat dynamic environment at the microscopic level. A balance prevails between tear fluid secretion and drainage (Palakuru et al. 2007). The main and accessory lacrimal glands secrete aqueous tears, with a small addition from the conjunctiva (Dartt 2009), and the tears are drained via the nasolacrimal system. An important fraction of the aqueous phase is also lost through evaporation (King-Smith et al. 2004). The blinking-reflex-provoked sweeping motion of the lids (mainly that of the upper lid) protects the exposed ocular surface by restoring an intact tear film lipid layer after each blink. During the sweeping motion, an aliquot of meibomian lipid is spread from the lid margin onto the aqueous layer of the tear film, where it forms the tear film lipid layer (Foulks and Bron 2003, Bron et al. 2004). Meibomian gland lipid production arises from the continuous secretory activity of the glands and from the squeezing action of the lids. The compression caused by the stroke of the lids and subsequent spontaneous expansion of the TFLL after opening the eye is well recognised; however, the extent of its reorganisation is somewhat unknown. The extent to which the aqueous phase is influenced by the blink is also unrecognised (Tiffany 1997, Owens and Phillips 2001). After the upsweep of the upper lid, the TFLL spreads upwards and proceeds with an initial velocity that logarithmically decays to zero (Owens and Phillips 2001, Goto and Tseng 2003). TFLL stabilises into a somewhat static state after approximately one second after a blink, after which the tear film starts to rupture if the eye is not blinked. Depending on the subject, the tear break-up time of a healthy eye ranges from a few seconds to 20 seconds (Nichols et al. 2002). In patients with ADDE or with a pathological corneal epithelium, tear break-up may occur already within the normal interblink period and therefore lead to the formation of a dry spot. The reasons for the tear break-up may be numerous, such as the excess evaporation of water from the ocular surface (King-Smith et al. 2009).

It was originally suggested that the lipid layer spreads over the aqueous layer in two stages (Holly 1973). (*i*) The polar lipids spread over the air-water interface in the wake of the lid upsweep, and (*ii*) the non-polar lipids subsequently spread over the polar lipids, driven by the hydrophobic interactions of the PL fatty acyl chains (Yokoi et al. 2008). The initial flow force driving the spreading of the lipids would therefore be the surface tension gradient across the cornea (Marangoni flow). A more modern theory of the tear film behaviour during and after blinking is that the lipid layer only folds and returns to the initial state in organised fashion without significant reformation or exchange of lipids (Bron et al. 2004).

2.5 Lipid monolayers

2.5.1 Surface tension and surfactants

Liquids with strong intermolecular forces, such as water with the characteristic hydrogen bonding, possess high surface tension. In short, the molecules at the liquid-gas interface experience differing attractive interactions with the neighbouring molecules relative to the molecules in the bulk of the liquid. This unfavourable energy state of the system induced by the high-energy boundary molecules is decreased by minimising the surface area relative to the volume of the liquid observed as a curvature of a water droplet. The high surface tension of water is observed, for instance, as poor wetting of surfaces.

Amphipathic molecules, such as lipids, decrease the surface tension of water. Specifically, PLs are efficient biological surfactants. These molecules adapt an orientation at the air-water interface in which the hydrocarbon chains point towards the gas phase and the hydrophilic head groups face the aqueous phase (Möhwald 1990). When the surface concentration of the PLs, i.e., the average distance between neighbouring molecules, reaches a certain lipid-specific threshold, the lipids start to interact with each other. The interactions of the neighbouring polar head groups are repulsive due to the charged phosphate and nitrogen groups, whereas at extremely short inter-molecular distances, the hydrocarbon chains form attractive van der Waals interactions between each other. However, the total interaction between the molecules is highly repulsive because the repulsive forces are considerably larger than the weak van der Waals interactions. Therefore, a high surface concentration of lipids is needed to force these molecules close to each other. The short distance between the repulsive molecules creates a collective lateral tension (pressure) that is opposite to the surface tension of the interface, thereby decreasing the curvature of the interface and aiding spreading of the liquid. The interactions between the acyl chains retain the orientation of the individual molecules and therefore the organised structure of the lipid layer under high lateral pressure. The lipid-monolayer-induced decrease in the surface pressure relative to the clean interface can be measured as surface pressure using a Langmuir film balance.

2.5.2 Co-operativity and phase transitions

Because polar lipids dissolve poorly in aqueous solutions, the high-energy state of the molecules drives the molecules into three-dimensional low-energy lipid aggregates, such as micelles and liposomes. The hydrophobic, electrostatic, and steric forces between neighbouring molecules mainly determine the form of the spontaneously formed lipid aggregates (Luisi et al. 2008). In addition to the cell bilayers and cell compartments, more specialised examples of this phenomenon are the lung surfactant and TFLL, which, despite their complex structures, are essentially monolayers.

A single lipid molecule cannot undergo a phase transition; instead, phase transitions in lipid membranes arise from the co-operativity of lipids. (Möhwald 1990). Lateral compression of the lipid monolayers causes a decrease in the area occupied by each lipid molecule. Therefore, the freedom of motion of a single lipid molecule decreases as the neighbouring molecules interact with each other. Compression of an expanded (gas-phase) lipid film results in organisation into a liquid-expanded (LE) phase. Under continuous compression, monolayers composed of certain, typically saturated PLs, transition from a LE phase to a liquid-condensed (LC) phase. The transition from the LE phase to the LC phase depends largely on the attraction of the acyl chains between the lipid molecules. As the transition proceeds, the configuration of the fatty acyl chains changes, as shown in Figure 4. This transition results in a trans-gauche rotational isomerisation of the acyl chains, observed as a decrease in the area occupied by a single lipid molecule and as an increase in the monolayer thickness due to a change in the acyl chain tilt angle. The LE-to-LC transition proceeds through the formation of LC domains that grow and fuse during compression. The domains may obtain various shapes and sizes depending on the interplay of line tension and electrostatic repulsion of the domains (Holopainen et al. 2001, Karttunen et al. 2009). Upon expansion of the monolayer, a reversible phase transition from a LC phase to a LE phase occurs.

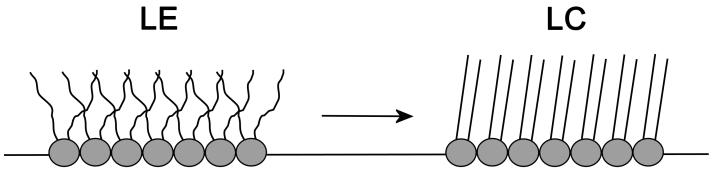

Figure 4. The acyl chains undergo a change in configuration during the phase transition from a liquid-expanded phase to a liquid-condensed phase. The increase in collective van der Waals interactions between the acyl chains results in a condensed collapse-resistant monolayer. Adapted from Rantamäki et al. 2011.

With increasing lateral pressure, the increased order of a lipid monolayer reaches a state in which the molecules cannot be accommodated in one layer. Consequently, the monolayer collapses, i.e., parts of the lipids are driven into coexisting three-dimensional aggregates instead of the two-dimensional monolayer. After collapse, the lateral pressure within the layer does not increase, i.e., the surface pressure reaches a plateau. Depending on the lipid species, the lipids may be displaced from the monolayer to bulky three-dimensional aggregates. During expansion of the layer, the aggregates may not spread reversibly, and this is detected in isotherms as hysteresis. A layer composed of certain lipids may fold in a more organised fashion and thus are more rapidly spread during expansion of the lipid layer. Lipids in the LC phase are more resistant to collapsing and may thus reach high surface pressures.

The behaviour of the lipid layer under lateral compression depends on the properties of the lipid species and on the surrounding environment. The magnitude of the attractive van der Waals forces between hydrocarbon chains is dependent on the length and saturation of the chains, which considerably affect the cross-sectional area of the molecule. For instance, unsaturated PLs, such as egg-yolk PC (eggPC), do not undergo a compression-induced LE-to-LC phase transition at physiological temperature because the kink formed by the double bond prevents the required interactions between the chains. Vice versa, saturated PLs, such as dipalmitoyl phosphatidylcholine (DPPC), readily undergo this phase transition.

In addition to the structural properties of the lipids, temperature has an effect on the phase transition behaviour of the monolayers. Lipids in the monolayer possess a characteristic phase transition temperature. The lipid layer undergoes a transition from a gel phase to a liquid crystalline phase when the temperature exceeds the phase transition temperature. This monolayer “melting point” is not necessarily equivalent to the bulk melting temperature of the lipid. The temperature-induced transition in the packing density of the lipid molecules is caused by the change in the thermal motion of the hydrocarbon chains and therefore affects the order of these chains in a very similar fashion to the LC-to-LE transition.

Additionally, minute variations in the lipid composition or changes in the pH and ionic strength (affecting the charge of the head groups) may result in significant changes in the physical behaviour of these lipid layers.

The complexity of the inter-lipid interactions increases considerably in lipid layers, which contain several lipid species. For instance, mixtures containing both polar and hydrophobic non-polar lipids tend to from multi-layered structures as a function of the molecular area. This increased complexity significantly complicates the investigation of such layers.

2.6 Organisation of TFLL

The TFLL is assumed to retain a somewhat stable organisation in response to the dynamic environment, which the sweeping lids create. The organisation is maintained whenever the lipid layer is capable of handling rapid area changes during compression by re-organisation of the lateral molecular packing and certain mechanism of folding. Equally important is the instantaneous re-spreading of the folded stage. The capability of the TFLL to reorganise arises from the composition of the layer. The molecular level organisation also affects the rheological behaviour of the TFLL.

2.6.1 Molecular level behaviour of TFLL

The number of studies aiming to explain the molecular organisation of the TFLL is very limited. Because of the partly unsolved composition of the tear film, there are two differing approaches to studying the molecular level behaviour of the TFLL *in vitro* – using either meibum or artificial TFLL-like compositions as the lipid layer models. Both of these options have their advantages and disadvantages.

2.6.1.1 Meibum studies

The behaviour of meibum at the air-water interface is typically studied using methods such as Langmuir film or pendant drop techniques. Interpretation of the results obtained from these techniques most often requires that the composition of the lipid layer is precisely known. Therefore, the analysis of the results obtained from these studies is very demanding due to the compositional complexity of the meibum, and the results may leave room for subjective interpretations. However, the advantage of the meibum studies is that the lipid composition represents the TFLL very closely.

Mainly based on the meibum studies and the composition of meibum, a novel model of the TFLL structure has been presented – a duplex film (Millar and King-Smith 2012, Rosenfeld et al. 2013, Cerretani et al. 2013). This model, as the name suggests, also consists of two layers, but it somewhat differs from the previous multi-layered structure (McCulley and Shine 1997). The second layer consists of unorganised bulky lipid phase overlaid on top of the organised layer located at the lipid-water interface. According to this model, the overlaying phase, possibly composed of molten WEs, is mainly in the liquid state at physiologic temperature, but it also contains ordered lamellar particles, most likely CEs, dispersed in the liquid phase.

2.6.1.2 TFLL-like compositions

TFLL-like compositions typically contain two to four lipid components selected based on the TFLL composition. The advantage is that the lipid layer typically only contains the main lipid classes contained by the TFLL, and due to the more simple composition, the results are easier to interpret and leave less room for subjective evaluation. Additionally, the limited number of lipid components allows molecular simulations to be performed as

supporting information. The disadvantage is that the lipid layer compositions do not entirely represent the composition of *in vivo* TFLL.

The lipid organisation and dynamics have recently been attempted to clarify with TFLL-like composition of 60% egg-yolk phosphatidylcholine (eggPC), 20% free fatty acids, 10% cholesteryl oleate (CO), and 10% triglycerides (TGs) (Kulovesi et al., 2010). The TFLL-like layer was compared to an eggPC monolayer using Langmuir-film balance techniques, X-ray diffraction, atomic force microscopy, and Brewster angle microscopy (BAM) and finally complemented by molecular simulations. The results suggest that a layered structure is formed as proposed originally by McCulley and Shine (1997); polar eggPC and free fatty acids are located at the air-water interface, and the non-polar layer of CO and TGs overlays the polar lipids. However, the organisation of this layered structure depends on surface pressure. With increasing surface pressure, the non-polar lipids were found to form tubular and round-like neutral lipid aggregates at the air-PL interface.

The near-atomistic molecular dynamics simulations showed that at low surface pressures, CO molecules and TG molecules were located between PLs and free fatty acids. With a gradual increase in surface pressure, COs and TGs diffused to the PL-air interface and formed a separate phase on a microscopic scale. These aggregates fused and finally formed a unified CO/TG phase. Simultaneously, the underlying PL/fatty acid monolayer folded towards the aqueous phase, forming a lipoprotein-like structure where non-polar lipids were enclosed by a PL monolayer. Another study (Kulovesi et al. 2012) with similar compositions concentrated on the impact of the non-polar lipids on the behaviour of the TFLL-like layer. The non-polar lipid proportion of ≤20%, namely the proportion of CO and TGs, seemed to increase the compressibility relative to the eggPC monolayer, whereas larger proportions resulted in excessive aggregation of the non-polar phase and, therefore, increased the instability of the layer.

2.6.2 Rheological properties of TFLL

TFLL is a viscoelastic lipid layer. Viscoelasticity is a physicochemical property, which allows dynamic films such as TFLL to resist deformations. Rheology studies quantitatively determine how materials that have viscous and elastic properties deform when stress is applied as a function of force, time, and spatial orientation (Janmey and Schliwa 2008). Elasticity describes the ability of the matter to return to the initial shape after the stress is removed, whereas viscosity describes the ability of the matter to flow. Typically, rheological properties are measured for bulk, i.e., three-dimensional, materials. This should be separated from surface rheological properties, which describe the rheological properties in two-dimensional systems such as monolayers. Therefore, the rheological properties of a bulk material do not apply when the same material is spread as a monolayer. The elasticity of a monolayer in two dimensions mainly describes how the monolayer restores (spreads) to the initial form when the deforming force is removed, whereas viscosity describes how motion is dampened in the layer (Yokoi et al. 2008).

The main deforming force affecting TFLL originates from the compression-relaxation cycles induced by the sweeping lids. The viscoelastic properties have been observed *in*

vivo using video-interferometric techniques (Yokoi et al. 2008, Goto and Tseng 2003). The main indication of TFLL viscoelasticity is detected post blink, when the lipid layer spreads over the air-tear interface restoring to the pre-blink form almost identically. This suggests that the TFLL possesses elastic characteristics. The viscous component of the behaviour is observed as a damping of the spreading motion towards the end of the spreading. Despite the rapid initial rate of spreading, the motion stops only after a period of approximately one second. In addition to the ability to fold and spread rapidly, the viscoelastic properties may play a significant role in stabilisation of the tear film during the inter-blink period, therefore retarding the tear film break-up (Rosenfeld and Fuller 2012).

Similar properties have been measured for meibum and artificial TFLL compositions *in vitro* (Kulovesi et al. 2010, Leiske et al. 2010, Kulovesi et al. 2012, Arciniega et al. 2013, Raju et al. 2013). However, the interpretation of the results and assessment of their physiological relevance has proven to be problematic.

2.7 Retardation of evaporation by lipid monolayers

The properties that affect the evaporation-retarding effect of one-component monolayers are well established (Barnes 2008). Typically, monolayers composed of polar lipids, such as fatty alcohols and fatty acids, which have a small head group and long saturated hydrocarbon chain, retard evaporation effectively. A common property of these monolayers is a low compressibility. The molecules organise into condensed lipid layers, even at low surface pressures, due to the small head group and low inter-molecular repulsion between these groups. The low compressibility is observed as a rapid increase in surface pressure when the lipid layer is compressed because very little reorganisation takes place in the monolayer. Fatty alcohol monolayers, for instance, decrease the evaporation by ~60% (La Mer and Healy 1965). The ability to control the diffusion of water molecules through the lipid layer is due to the attractive van der Waals interactions between hydrophobic hydrocarbon chains because the free volume between the molecules is very low (Patra et al. 2006). The evaporation-retardant effect increases with increasing surface pressure due to the decrease in hydrocarbon chain tilt and the resulting increase in monolayer thickness before reaching a lipid-species-dependent plateau (Henry et al. 2010). With mixed monolayers containing two evaporation-retarding lipids, the total evaporation resistance is the sum of their individual resistances (Rosano and La Mer 1956).

The mechanistic knowledge of the potential evaporation-retarding effect of TFLL is very limited. The theory of an evaporation-retarding TFLL originates from the *in vivo* evaporation rate measurements, which show that the evaporation from the ocular surface is multiple orders of magnitude slower than from an air-water interface *in vitro* (Borchman et al. 2009). However, the problematic aspect with *in vivo* measurements is that the evaporation rate cannot be measured without the TFLL to define the total effect of the TFLL on evaporation in the entire tear film structure. Few studies have investigated the evaporation-retarding effect of the TFLL-like layers *in vitro*, and the

potential mechanism behind evaporation-retarding TFLL is still unclear. According to *in vitro* studies, meibum layers result in a reduction of only 6% to 8% in the evaporation rate at near-physiologic temperatures (Herok et al. 2009, Cerretani et al. 2013).

2.8 TFLL and lung surfactant

TFLL and pulmonary surfactant share several similar properties (Rantamäki et al. 2011). Whereas TFLL covers the aqueous layer lining the ocular surface, pulmonary or lung surfactant covers the aqueous hypophase lining the alveolar epithelium. Tear fluid as well as lung surfactant and the underlying hypophase both contain a variety of lipids and proteins, and they have a distinct structure, which defines their respective functions. Both films consist of an aqueous layer lining the epithelium and an anterior lipid layer at the air-water interface. The films function in a very dynamic environment due to the blinking of the eye and expansion-contraction breathing cycle of the alveoli in lungs.

The function of the surfactant is to control the surface tension of the alveolar epithelium (Notter 2000). Because lungs contain alveoli of different sizes, different pressures are needed to inflate them. Without the lipids at the air-water interface, an alveolus with a large radius has a lower surface tension than an alveolus with a smaller radius, and thus, the two require different pressures to inflate. The lipid layer adjusts the surface tension as a function of the alveolar radius, thereby fully inflating all the alveoli at differing pressures and preventing collapse or over inflation. The reduced surface tension also decreases the pressure needed to inflate the lungs, thereby allowing easier breathing.

2.8.1 Lipid composition of lung surfactant

Lung surfactant contains 85-90% (w/w) of PLs, 4-7% of non-polar lipids, and 6-8% of proteins (Notter 2000). The lung surfactant is synthesised by epithelial alveolar type II cells and stored and secreted by exocytosis from the lamellar body organelles located in the cytoplasm of these cells. In the hypophase, the surfactant components form heterogeneous protein-lipid aggregates, such as tubular myelin. From these aggregates, the components of the lipid layer are adsorbed to the surface. Type II cells also take up the surfactant by endocytosis; components may be used again for the synthesis of new surfactant or may be recycled. The half-life of the lung surfactant varies from a few hours to 30 hours depending on the surfactant component and the age and species of the subject (Ikegami and Jobe, 1998).

The most abundant PL class is PC, constituting ~80% (w/w) of all PLs (Veldhuizen et al. 1998). DPPC comprises 40-50% of all PCs and, therefore, one-third of the total PLs. Other abundant PLs in mammals are phosphatidylglycerol (~10% of total PLs) and, in humans, PE ~12% (other mammals only 2% to 5%). In all mammals, lysoPC, phosphatidylinositol, phosphatidylserine (PS), and SM are also found in small amounts.

The most profuse non-polar lipid is cholesterol, which comprises 80-90% of all non-polar lipids and ~4% of the total lipids (Veldhuizen et al. 1998). Minor lipids are CEs, free fatty acids, and mono-, di-, and triacylglycerols.

2.8.2 Protein composition of lung surfactant

The proteins involved in the organisation and function of the lung surfactant lipid layer are better known than the similar proteins in the tear film. Lung surfactant contains four surfactant proteins (SP) named SP-A, SP-B, SP-C, and SP-D (Johansson et al. 1994). SP-A comprises approximately half of the total protein mass of the surfactant proteins, whereas SP-B, SP-C, and SP-D each account for less than 1%. SP-A, SP-B, SP-C, and possibly SP-D facilitate the trafficking of lipids between the monolayer/bilayer structures at the interface and tubular myelin structures (Notter 2000). The tubular myelins are microstructures composed of lipid bilayers and proteins, and they act as lipid storage in the lung surfactant hypophase. The proteins aid the transport and adsorption of the lipids by disrupting and fusing the lipid structures and also function as organising components in these structures.

Interestingly, both fluids share a number of lipid-interacting proteins, such as lipocalins (Glasgow et al. 1995, Wattiez et al. 2000, Merkel et al. 2005), lipophilin (Lehrer et al. 1998), PLTP (Albers et al. 1995, Jiang et al. 1998, Jauhiainen et al. 2005), and surfactant proteins A, B, C, and D (Brauer et al. 2007, Brauer et al. 2007), which suggests that such proteins may be involved in maintaining homeostasis in both films.

Proteins involved in the defence response, immune response, stress response, and proteolysis are well represented in both fluids, as illustrated in Figure 5 presenting the relevant biological processes (de Souza et al. 2006, Gharib et al. 2009). This emphasises the importance of host defence in both fluids. However, there are also notable differences: lung surfactant contains a large number of proteins involved in cell adhesion and motility as well as programmed cell death, whereas a large proportion of proteins in tear fluid are involved in bacterial defence and inflammatory-response proteins, indicating the intimate interaction between the ocular surface and surrounding pathogens.

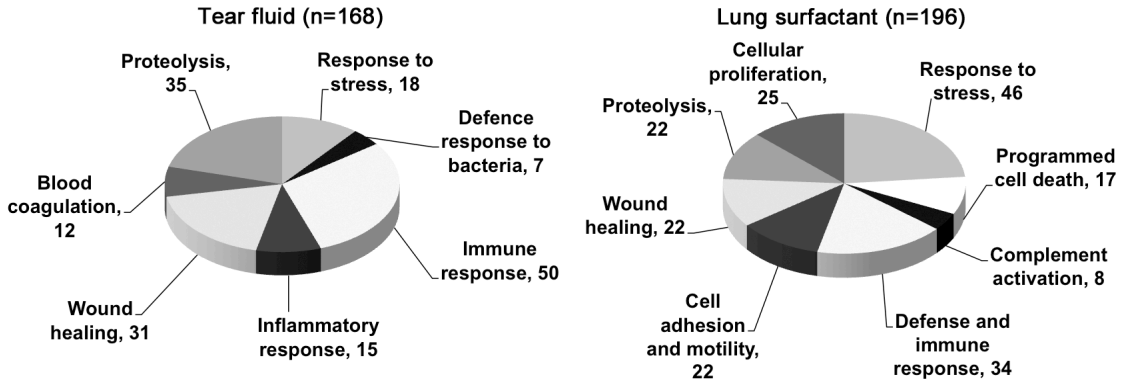

Figure 5. The relevant biological processes in tear fluid (de Souza et al. 2006) and lung surfactant (Gharib et al. 2009). The numbers designate the number of proteins in each group; n designates the total number of proteins investigated. Adapted from Rantamäki et al. 2011.

2.8.3 Surface activity of lung surfactant

The lung surfactant is able to reduce surface tension to very low values. The underlying molecular mechanism for producing low surface tensions is not completely understood, but it may be due to the high content of DPPC in lung surfactant (Notter 2000). At small molecular areas, i.e., high surface concentration of lipids, a DPPC monolayer produces surface pressures of over 70 mN/m, i.e., surface tensions below 1 mN/m. At low molecular areas, the saturated DPPC monolayer transitions from LE phase to LC phase – a highly viscous solid-like state that explains the collapse resistance of a DPPC monolayer (Yan et al. 2007). As described by a classical model, the lateral compression of a mixed DPPC-containing monolayer at low molecular areas causes "the squeeze-out" of fluid-like non-DPPC components and results in enrichment of the monolayer with solid DPPC (Zuo and Possmayer 2007).

Because the experimental studies regarding surfactant behaviour are challenging, molecular simulations have been used to complement experiments. At extremely low molecular areas, the surfactant layers begin to fold in an organised fashion. Based on the simulation, instead of taking place at the air-lipid interface, the folding occurs at the lipid-water interface below the monolayer (Baoukina et al. 2007). At high surface concentrations, the lipid monolayer folds into bilayer structures finally forming liposome-like structures (Baoukina et al. 2008). In contrast, the amphipathic layer of the TFLL folds towards the aqueous phase and the accompanying non-polar lipids phase separate forming lipoprotein-like structures at the lipid-air interface.

2.8.4 Composition defines the functions of TFLL and lung surfactant

To conclude, the lipid composition plays a necessary role in the function of tear film and lung surfactant (Rantamäki et al. 2011). The main function of the tear film lipid layer is to reduce surface tension and to reduce evaporation of the tear fluid, whereas the main function of lung surfactant is to reduce surface pressure effectively to close-to-zero values. Tear fluid and lung surfactant both contain polar lipids, mainly PLs, and non-polar neutral lipids. The essential difference between these lipid layers is the relative proportions of these two lipid groups. Lung surfactant contains mainly PLs and less than 10% of non-polar lipids. In contrast, TFLL contains, in addition to PLs, a substantial proportion of non-polar lipids. The differing compositions define the molecular organisation of the lipid layers, and plausibly, the proteins also affect the organisation of the lipids. While lung surfactant is mostly a monolayer, it also contains multilayer regions possibly caused by a collapsed monolayer and adsorption of lipids from the hypophase. In contrast, TFLL consists of a polar lipid layer at the air-water interface accompanied by the overlaying non-polar lipid layer. The differences in the composition and structure also result in differing folding/re-spreading behaviour under the characteristic compression-expansion cycles the layers undergo *in vivo*.

3. AIMS OF THE STUDY

The aim of this thesis project was to study the composition and structure of the tear film lipid layer using *in vitro* methods and to uncover more details of TFLL function, particularly the potential evaporation-retarding effect of the layer.

The specific goals were as follows:

1. Reveal the lipid composition of human tear fluid, and specifically, demonstrate that phospholipids exist in human tear fluid. A secondary goal was to illustrate a plausible function for the phospholipids in the TFLL.
2. Study the evaporation-retarding effect of TFLL-like lipid layers *in vitro*.
3. Investigate in more detail the evaporation-retarding effect of a specific TFLL lipid class: wax esters.

4. METHODS

4.1 Tear fluid samples

The experiments on the human tear fluid samples were performed according to the guidelines of the Declaration of Helsinki. The Ethical Committee of the Helsinki-Uusimaa Hospital District approved this research. Written informed consent was obtained from each subject. Glass micropipettes (5 μL, Blaubrand Intramark, Brand GmbH, Wertheim, Germany) were used to collect tear samples from the lower conjunctival sac of 30 healthy volunteers (age 20–55 years). The tear collection under a biomicroscope was performed during multiple sessions causing the least possible irritation of the conjunctiva to minimise cellular contamination and reflex-tearing-induced sample dilution. The samples were instantly cooled to +4 °C, centrifuged at 13 000 rpm for 5 min to remove any possible cellular debris contamination, and the collected supernatant was stored at -20 °C until analysis. Cellular contamination of the sample pools was controlled by Western blotting using anti-actin rabbit polyclonal antibodies (Sigma-Aldrich, St. Louis, MO, USA). Corneal epithelial cell lysate was used as a positive control.

4.2 Sample pre-treatment

For thin layer chromatography (TLC), lipids were extracted from ~80 μL of tear fluid using an adapted Folch method (Folch et al. 1957). In short, the proteins were precipitated from the tear fluid sample by addition of a chloroform-methanol solution. Then, the lipids were extracted from the supernatant so that the total composition of the solution (including the supernatant from the precipitation) was 8:4:3 chloroform/methanol/water (v/v). The aqueous phase was extracted with a chloroform/methanol/water (68:14:1) solution, and the organic phases from both extractions were combined. The solvent was evaporated, and the extracted lipids were dissolved in chloroform. The sample was divided into two aliquots and applied to thin TLC Silica gel 60 glass plates (Merck KGaA, Darmstadt, Germany).

For mass spectrometric analysis, tear samples collected from the subjects were pooled into two separate samples for lipid composition analysis. The pooled tear samples (2x75 μL) were spiked with 20 μL of a standard mixture containing ten lipid class standards (lysoPC, PC, PE, PS, phosphatidic acid, phosphatidylglycerol, ceramide, monoacylglycerol, diacylglycerol, and TG as their heptadecanoic derivatives) at levels of 0.18–0.22 μg. Lipids were extracted with 100 μL of chloroform:methanol (2:1) by vortexing for 2 min at room temperature. Following 1 hour of incubation, the samples were centrifuged at 10 000 rpm for 3 min, and the lower organic solvent layers were separated into glass vials containing another lipid standard mixture (labelled lysoPC, PC and TG standards at a level of 0.1 μg). The samples were evaporated to dryness and dissolved in 20 μL of chloroform:methanol (2:1). The ratios between the unlabelled and

labelled standards were used to control the extraction procedure. In the sample set, non-extracted and extracted standard samples were also included to assess the validity of the extraction.

4.3 Lipid analysis

4.3.1 Enzymatic assays

The concentrations of total cholesterol (Roche Diagnostics GmbH, Mannheim, Germany), choline-containing PLs (DiaSys Diagnostic System GmbH, Holzheim, Germany) and TGs (Roche Diagnostics) in pooled tear fluid samples were determined using enzymatic assays. A Victor2 1420 Multilabel Counter (Wallac Corp., Turku, Finland) was employed for the absorbance measurements. The respective assays for each class were performed twice.

4.3.2 Thin layer chromatography

TLC separations were performed for both polar and non-polar lipids. The eluent for polar lipid separation comprised 70:20:12:4:2 chloroform/methanol/acetic acid/formic acid/water and for non-polar lipids 80:20:1 hexane/diethyl ether/acetic acid. Following the separation, the plates were incubated in a solution containing 3% (w/w) copper sulphate and 8% (w/w) phosphoric acid and heat treated by raising temperature from ambient room temperature to 180 °C during 30–45 min. The charred lipids were detected from the plates by visual inspection and identified by comparison to proper lipid standards. The separation was performed for two pooled samples.

4.3.3 Ultra performance liquid chromatography – mass spectrometry (UPLC-MS)

The extracted lipids were analysed on a Waters Premier quadrupole time-of-flight (Q-TOF) mass spectrometer (MS) combined with an Acquity ultra performance liquid chromatograph (UPLC). The separation was performed at 50 °C in an Acquity UPLC^{TM} BEH C18 2.1x100 mm column with 1.7 mm particles. The injected sample volume was 2.0 µL (Acquity Sample Organizer). The gradient eluent system consisted of component A: ultrapure water (1% 1 M NH_4Ac, 0.1% HCOOH) and component B: LC/MS grade acetonitrile/isopropanol (1:1 (v/v), 1% 1 M NH_4Ac, 0.1% HCOOH). The gradient composition changed from 65% A/35% B to 80% B in 2 min, followed by 100% B in 7 min, and finally remained at this composition for 7 min. The column was re-equilibrated for 4 min before the next run. The flow rate was 0.4 mL/min. Reserpine was utilised as the lock spray reference compound. The lipid profiling was performed in ESI+ mode, and the data were collected at m/z range of 300–1200 with a scan duration of 0.2 s. The

data processing was carried out using MZmine 2 software (Pluskal et al. 2010), and the lipids were identified according to an internal spectral library (Yetukuri et al. 2007).

4.4 Spreading experiments

4.4.1 Langmuir-Blodgett technique

Samples for contact angle measurements were prepared using the Langmuir-Blodgett technique, i.e., a lipid monolayer from an air-water interface was transferred to a solid support. The freshly cleaved mica sheets (Agar Scientific Ltd, Stansted, UK) were vertically submerged through an air-water interface utilising a Langmuir balance unit (Minitrough, KSV Instruments Ltd., Helsinki, Finland). EggPC in 1 mM chloroform solution was applied to the interface. Preceding the transfer, the monolayer was compressed and relaxed twice to the transfer surface pressure of 20 mN/m or 30 mN/m. The transfer was performed at constant surface pressure by elevating the mica substrate through the air-water interface at 2 mm/min. The transfer ratio from the air-water interface to the mica support was approximately 1:1.

4.4.2 Contact angle measurements

The contact angles were measured using a CCD-camera-based contact angle meter (CAM 200, KSV Instruments Ltd., Helsinki, Finland). The contact angles were determined in the CAM200 software by using a fitting method based on the Young and Laplace equation. The liquid for which the contact angles were determined was commercial extra virgin olive oil composed of 10% (w/w) saturated, 80% monounsaturated and 10% polyunsaturated fatty acids. Olive oil is mainly composed of TGs and small amounts of free fatty acids, and therefore, it was used as a simple model substance replicating the non-polar lipids of the TFLL. An aliquot of olive oil was applied to the mica surface with a threaded plunger syringe (Hamilton Co., Reno, USA). The volume of the drop hanging on the needle was increased gradually until the drop detached from the tip. The camera automatically recorded 21 images every 33 ms and then 39 images at one image/second. The contact angles were defined in 0.1, 0.2, 0.3, 0.4, 0.7, 1.7, 4.7, 9.7, and 39.7-second intervals. A minimum of six contact angles were measured for each time point using two duplicate samples (3 drops per sample). The values are expressed as the mean ± standard deviation.

4.5 Melting point determination

The WE melting points (MPs) were determined using a Stuart SMP10 melting point apparatus (Bibby Scientific Ltd, Staffordshire, UK). The temperature was elevated 2 °C/min until the melting transition was observed. The temperature accuracy of the apparatus at 20 °C was ±1 °C. The MP of each solid state WE (MP >25 °C) was determined four times.

4.6 Evaporation rate determination

Evaporation rates were measured using a custom-built system. The system was built around a Langmuir balance unit (KSV Instruments Minitrough, Helsinki, Finland) with a trough area of ~273 cm^2. The temperature of the trough was controlled using an external heating thermostat (Lauda Eco E4, Königshofen, Germany). The temperature of the subphase was determined with a thermometer connected to the Langmuir balance unit. The unit was enclosed inside a poly(methyl methacrylate) cabinet. An airflow of dried and filtered air was used to remove humid air from the cabinet and, therefore, to diminish the effect of ambient humidity variations on the evaporation rate. To adjust the flow of air through the cabinet, an approximate air mass flow was determined using an airflow meter (Testo 410-1, Lenzkirch, Germany). The relative humidity inside the cabinet was measured using a digital hygrometer (Testo 608-H1, Lenzkirch, Germany).

The evaporation rate determination was based on the evaporated mass of the subphase (phosphate buffered saline, PBS). The subphase mass was measured preceding the evaporation measurement. The subphase was placed into the trough, the lipid was applied in 10 mM chloroform solution to the air-water interface, and the surface pressure was measured with the Langmuir balance. The Wilhelmy plate was removed, and the front door of the cabinet was closed 10 min after the start. After 90 min, the trough was emptied, and the subphase was weighed again. For mass-to-volume conversions, a density of 1 g/mL was used for PBS.

4.7 Brewster angle microscopy

A KSV NIMA microBAM and KSV Mini trough (Helsinki, Finland) unit were used to observe the spreading and interfacial organisation of lipid layers at 35 °C. The lipids were applied to the air-water interface in 10 mM chloroform solution. Two differing methods were used in studies II and III. In study II, lipids were applied to the interface, the layer was compressed at a barrier speed of 10 mm/min, and images were captured at specific surface pressure points. In study III, to replicate the prevailing conditions during evaporation experiments, no compression was performed, and the spreading of the lipid layer was merely observed over a period of 15 min.

4.8 Langmuir film experiments

A Mini trough Langmuir balance unit (KSV Instruments, Helsinki, Finland) was used to record compression isotherms for WE layers at 35 °C. The lipid in 10 mM chloroform solution was applied to the surface of the PBS subphase. The lipid layer was compressed and relaxed at a rate of 10 mm/min five times until either a 45 mN/m surface pressure was achieved or the barrier reached the stopper. The amount of the lipid applied to the interface was adjusted so that the maximum compression could be achieved on the fifth cycle starting from ~0 mN/m.

4.9 Statistical methods

In study I, Student's t-test was employed to define the statistical significance between contact angles determined on a blank mica surface and on eggPC-coated mica. In studies II and III, a one-way ANOVA was employed to determine the statistical significance between the evaporation rate from the pure air-water interface and the evaporation rates through the lipid layers at the air-water interface. With both methods, a $p<0.05$ was considered significant.

5. RESULTS

5.1 Tear fluid lipid composition

5.1.1 Tentative lipid composition

We investigated the lipid composition of the tear fluid using TLC and enzymatic assays. We performed two separations for polar and non-polar lipids. We detected only very faint bands that, based on the elution distance, may have corresponded to SM (not shown). The separation for non-polar lipids showed a strong band eluting to an almost identical distance to that of a CE standard CO (Figure 6). We also detected faint bands eluting a similar distance as that of TGs and free cholesterol. The enzymatic assays resulted in concentrations of 48±14 μM for choline-containing PLs, 10±0 μM for TGs, and 21±18 μM for total cholesterol.

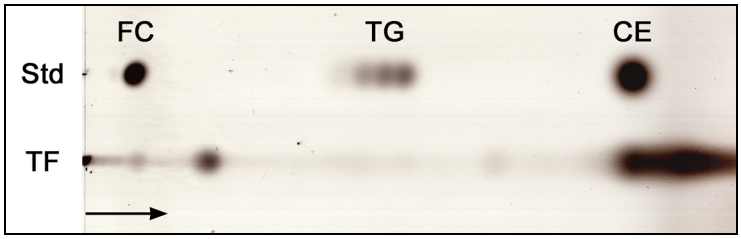

Figure 6. Thin layer chromatographic separation of the tear film non-polar lipids. Arrow designates the direction of eluent flow. FC, free cholesterol; TG, triglyceride mixture; CE, cholesteryl ester

5.1.2 Lipids identified by UPLC-MS

Based on UPLC-MS analysis, a total of 153 lipid species in six lipid classes were identified. Table 1 presents the concentrations of those six classes in tear fluid. Figure 7 illustrates the molar proportions (mean ± standard deviation) for the five most abundant lipid classes among the identified lipids. Polar lipids PC and PE comprised 69±12% (mol/mol) and 19±7% of all identified lipids, respectively. The remaining proportion contained 6±3% non-polar TGs, 3.3±1.2% SMs, and 3.4±1.8% ceramide.

The ten most abundant lipids ((lysoPCs (16:0), (18:1), (18:3), and (18:0); ether PEs (34:4) and (32:6); PEs (36:3) and (32:3); PC (36:3); and SM (d18:1/16:0)) comprised together 66±8% of all identified lipids. Unsaturated lipids covered 54±11% of all identified lipids. No free cholesterol or CEs were detected.

Table 1. The molar concentration of the identified tear film lipid classes based on the data obtained form UPLC-MS analysis.

CLASS	S1 (µM)	S2 (µM)	mean (µM)	SD (µM)
PC	13.8	28.0	20.9	10.1
PE	5.3	5.2	5.2	0.1
TG	1.7	1.3	1.5	0.3
Cer	1.1	0.8	0.9	0.2
SM	0.9	0.9	0.9	0.1
PS	0.1	0.1	0.1	0.01
TOTAL	22.9	36.3	29.6	9.5

Cer, Ceramide; PC, phosphatidylcholine; PE, phosphatidylethanolamine; PS, phosphatidyl-serine; SM, sphingomyelin; TG, triglyceride; TOTAL, total lipid concentration.

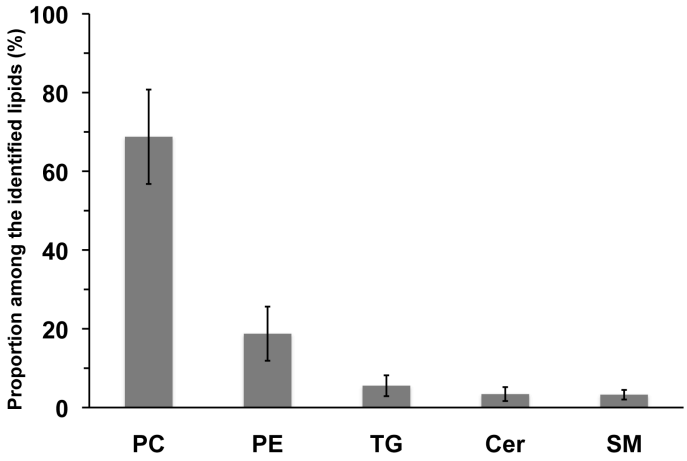

Figure 7. Molar proportions of the five most abundant lipid classes as identified by UPLC-MS. Cer, Ceramide; PC, phosphatidylcholine; PE, phosphatidylethanolamine; SM, sphingomyelin; TG, triglyceride.

5.2 The impact of phospholipids on spreading

We hypothesised that polar lipids are required to facilitate uniform spreading of nonpolar lipids in the TFLL and demonstrated this phenomenon by a simple macroscopic experiment. A hydrophilic mica sheet was coated with a monolayer of eggPC, which represented a situation in which PLs were spread as a monolayer at the air-water interface. Olive oil was the model substance for non-polar lipids, whereas un-coated mica represented a blank air-water interface.

Figure 8 visually illustrates the spreading of olive oil to a blank and eggPC-coated mica interfaces. Figure 9 shows the change in the contact angle as a function of time

during the first 4.7 s of spreading. At 0 s, the contact angle of a drop of olive oil on the blank interface was somewhat larger than on the eggPC-coated interface. At 0.1 s, the difference was more pronounced; the contact angles on the eggPC and blank mica interfaces were 57±2° and 71±6°, respectively. At 0.7 s, the spreading on the blank interface had stopped, whereas on the eggPC surface, the spreading continued. The minimum contact angles of 22±2° and 24±1° at respective surface pressures of 20 mN/m and 30 mN/m were significantly smaller compared to the minimum value of 45±1° on the blank surface.

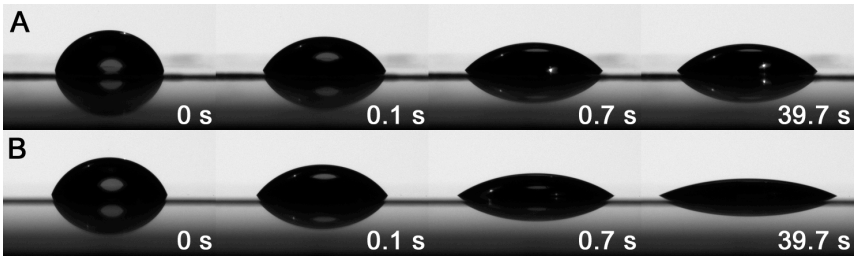

Figure 8. A photo sequence illustrating olive oil spreading on (A) blank mica and (B) on eggPC –coated mica.

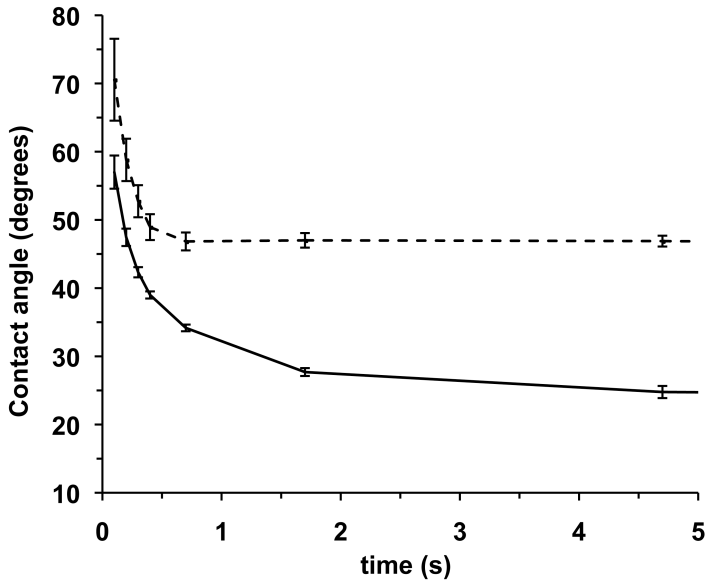

Figure 9. Olive oil spreading illustrated as contact angle vs. time. Dashed line, blank mica; solid line, eggPC-coated mica (N=6)

5.3 Melting points of wax esters

At room temperature, the WEs possessed three states: liquid, plastic wax, and powder. The MPs (Table 2) clearly followed the dependence on length and saturation of the hydrocarbon chains; lignoceryl lignocerate (LL) possessed the highest and behenyl arachidonate possessed the lowest MP.

5.4 Retardation of evaporation

The evaporation rate from the clean PBS interface at 35 °C was 10.90±0.12 μm/min (mean ± standard deviation) in study II and 11.2±0.3 μm/min in study III. In both studies, the respective values were set as reference evaporation rates. The performance of the system was controlled measuring evaporation rate through the behenyl alcohol (BAl) monolayer, which effectively retards evaporation. The decrease in evaporation rate induced by BAl was 45±2% in study II and 62±6% in study III. The results are given as a value ± propagation of uncertainty (based on evaporation rate standard errors). Additionally, at the reference temperatures of 30 °C and 41 °C in study III, PBS evaporation was 7.9±0.2 μm/min and 16.58±0.04 μm/min, respectively. The reduction in evaporation induced by BAl was 41±3% at 30 °C and 63±1% at 41 °C. Additionally in study II, a thick layer of olive oil (corresponding to thickness of 180 μm, if uniformly spread) was applied at the air-water interface to illustrate that macroscopic layers of oil retard evaporation. The decrease in evaporation rate induced by olive oil was 54±12%.

5.4.1 Evaporation retarding effect of one-component and TFLL-like layers

Simple PC monolayers did not decrease evaporation, whereas the evaporation rate through behenyl oleate (BO) layer decreased by 22.9±0.9%. This effect was maintained when BO was mixed with 10% (mol/mol) eggPC (1:9 PC/BO, 22.0±0.3%); however, lipid layers containing 40% and 90% of PC mixed with BO did not retard evaporation. The four component mixtures, PC/CO/TG/BO in ratios of 4:2:2:2, 1:3:3:3, and 1:1:1:7, were selected based on the lipid composition of study I, the composition of meibum, and the molecular level studies of similar compositions (Kulovesi et al. 2010, 2012). These compositions, however, did not demonstrate a significant decrease in evaporation rate. In summary, BO and 1:9 PC/BO layers decreased evaporation significantly compared to the clean PBS interface ($p<0.001$). However, the TFLL-like multi-component mixtures did not retard evaporation.

Table 2. The wax esters investigated in study III, structures, melting points (±1 °C), and evaporation-retarding effects at 35 °C and as a reference, for selected wax esters, at 30 °C and 41 °C.

Wax ester	Structure (FAl/FA)	MP (°C)	$RE_{35\,°C}$	$RE_{30\,°C}$	$RE_{41\,°C}$
Linolenyl oleate	18:3/18:1	<22	-		
Lauryl oleate (LO)	12:0/18:1	<22	-		
Myristyl oleate	14:0/18:1	8*	-		
Palmityl oleate	16:0/18:1	17*	-		
Stearyl oleate	18:0/18:1	24*	-		
Behenyl arachidonate	22:0/20:4	27	-		
Arachidyl oleate (AO)	20:0/18:1	33	-	++	-
Behenyl linolenate (BLNN)	22:0/18:3	36	+	+++	-
Behenyl linoleate (BLN)	22:0/18:2	37	++	+++	-
Behenyl oleate (BO)	22:0/18:1	38	++	-	-
Behenyl palmitoleate (BP)	22:0/16:1	38	+++	+	-
Behenyl laurate (BL)	22:0/12:0	54	-		
Behenyl myristate	22:0/14:0	58	-		
Behenyl palmitate	22:0/16:0	63	-		
Behenyl stearate	22:0/18:0	67	-		
Behenyl arachidate	22:0/20:0	73	-		
Behenyl behenate	22:0/22:0	75	-		
Behenyl lignocerate	22:0/24:0	77	-		
Lignoceryl lignocerate (LL)	24:0/24:0	79	-		

The positive/negative comparison is based on the retardation of evaporation within each temperature point. Negative sign designates a decrease of <10% in evaporation rate relative to the evaporation rate from pure interface. Abbreviations for selected WEs are given in the parenthesis. FA, fatty acid, FAl, fatty alcohol, MP, melting point; RE, retardation of evaporation.
WEs above upper dashed line, low MP
WEs between dashed lines, MP in near-physiologic temperature
WEs below lower dashed line, high MP
*Iyengar and Schlenk 1969

5.4.2 Evaporation-retarding effect of wax ester layers

Due to the evaporation-retarding effect of behenyl oleate, a series of additional 18 WEs were investigated in study III. The evaporation-retarding effects of these WEs are presented in Table 2 as a positive/negative comparison. Figure 10 illustrates the decrease in evaporation for the positive control BAl and the five evaporation-retardant WEs discovered in this study. At 35 °C BO, behenyl palmitoleate (PB), behenyl linoleate (BLN), and behenyl linolenate (BLNN) retarded evaporation. BP was the most effective evaporation retardant decreasing evaporation by 39±3%, whereas BO and BLN shared very similar evaporation-retarding effects decreasing evaporation by 30±2% and 27±2%, respectively. BLNN was the most inefficient evaporation-retardant decreasing evaporation by 20±1%. In turn, at 30 °C BLN and BLNN were the efficient retardants decreasing evaporation by 51±10% and 52±4%, whereas BP and BO decreased evaporation by only 12±1% and 5.2±0.2%, respectively. In addition to these four WEs, arachidyl oleate (AO) decreased evaporation by 16±1%. At 41 °C, these five WEs decreased evaporation by only 2.3% to 3.6%. The WE layers, excluding BO at 30 °C, decreased evaporation significantly compared to the blank PBS interface ($p<0.05$).

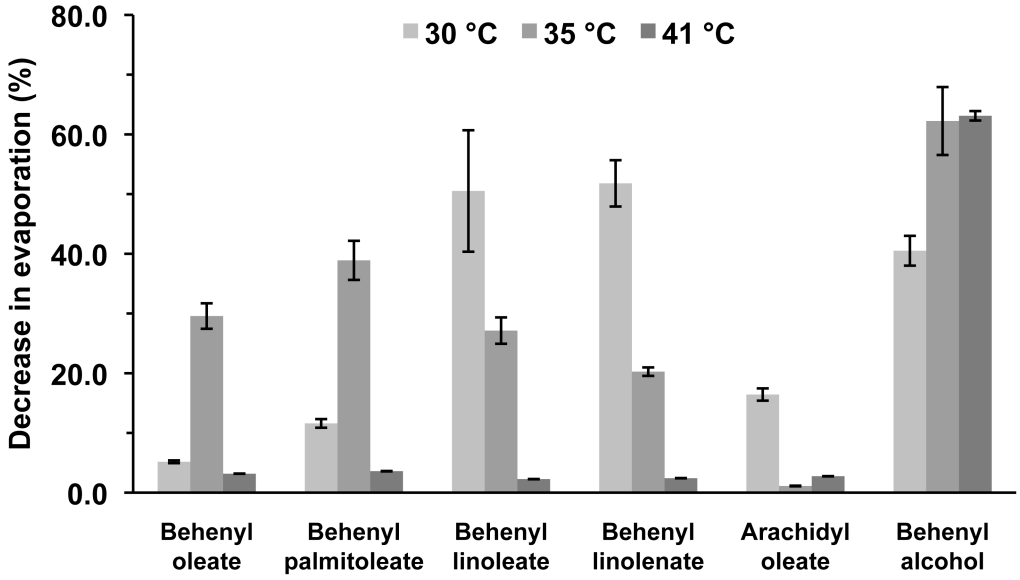

Figure 10. Lipid-layer-induced decrease in evaporation rate relative to the evaporation from PBS interface. Behenyl alcohol is the positive control. (N=3)

5.5 Interfacial organisation of TFLL-like layers

5.5.1 Interfacial organisation of mixed monolayers

In study II, the BAM images (Figure 11) illustrate the impact of increased non-polar-lipid proportion, and specifically, the increased proportion of behenyl oleate, on the appearance of the lipid layer. In the BAM images, black shades correspond to fluid monolayers, whereas grey shades correspond to gel-like condensed phase. Intense grey shades fading to white designate the formation of layers elevating from the lipid layer. The 4:2:2:2 layer seems noticeably more fluid than the aforementioned layers, as suggested by the dominant black shade. With increasing non-polar lipid proportion, the area of grey-shaded condensed lipid seems to increase. In the non-retardant PC/CO/TG/BO 1:3:3:3 and 1:1:1:7 layers, the total sum of the non-polar lipid species (CO/TG/BO) is equal, and this shows as similar areas of condensed phase lipid in BAM images. However, the evaporation-retardant PC/BO 1:9 forms a virtually uniform grey-shaded lipid layer, suggesting that the layer is in condensed phase.

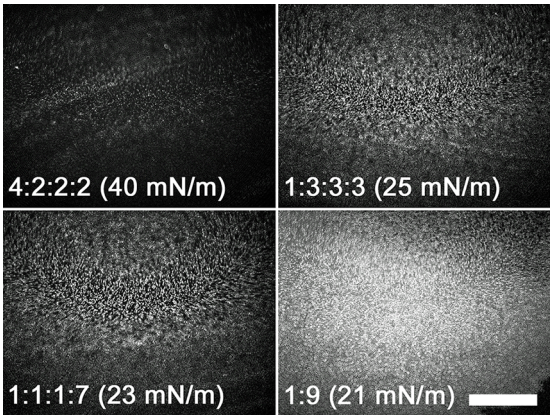

Figure 11. BAM images of selected multi-component TFLL-like lipid layers. Four-component mixtures contained PC/CE/TG/BO and the two-component mixture consisted of PC/BO. Scale bar is 1000 μm.

5.5.2 Interfacial organisation of wax ester layers

In study III, the WE layers were imaged with BAM (Figure 12) in conditions, which were virtually the same as in the evaporation experiments. The positive control BAl formed a uniformly spread layer, which was in a condensed phase as implied by the grey shade barely visible in the left lower-exposure image, but more evident in the right-hand-side high-exposure image. The images of BO, BLN and BLNN layers and the accompanying surface pressure information (3.3-3.7 mN/m) suggest that the lipid layer spread on the entire surface. The images also illustrate a large number of white shade

aggregates (in constant parallel movement during imaging) mixed with the black-shade liquid-phase lipid layer. The BP layer spread rapidly and resulted in a similar surface pressure (4.3 mN/m) as the three aforementioned evaporation-retardant WEs but appeared more layered (white shades), more condensed (grey shades), and virtually stagnant during the 15 min imaging period. The liquid-state-lipid lauryl oleate (LO) formed a uniform fluid layer with very little aggregation and high surface pressure (5.9 mN/m). In contrast, the LL layer appeared extensively aggregated, most likely due to the solid state of the bulk lipid. In addition, the surface pressure of 0.2 mN/m suggests that very little spreading occurred.

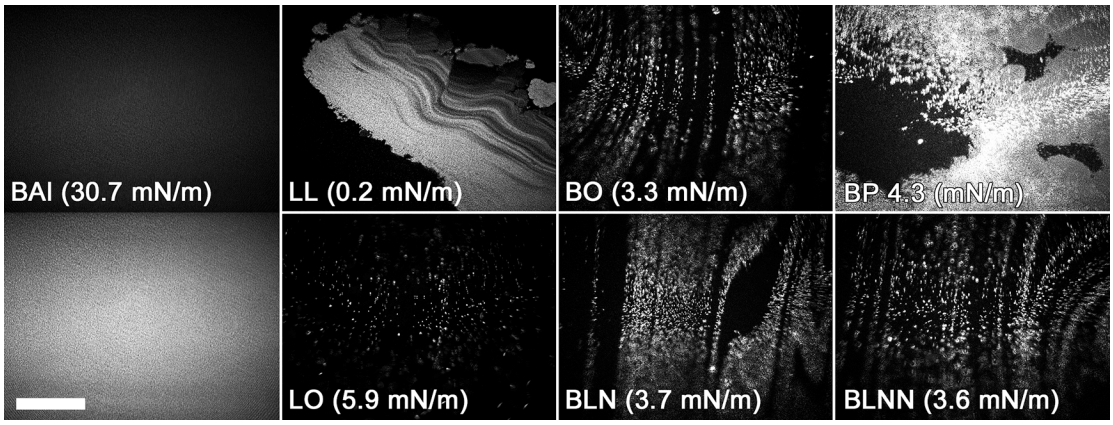

Figure 12. BAM images of BAl and selected WE layers at 35 °C. The exposure settings are the same in each image excluding the lower BAl image captured using higher exposure, and the LL image captured using lower exposure. Differing exposures were utilised to reveal more details. Scale bar is 1000 μm. BAl, behenyl alcohol; BLN, behenyl linoleate; BLNN, behenyl linolenate; BO, behenyl oleate; BP, behenyl palmitoleate; LL, lignoceryl lignocerate; LO, lauryl oleate.

5.6 Surface activity and dynamic stability of wax ester layers

We investigated the surfactant properties and dynamic stability of the WE layers using a Langmuir balance unit. Figure 13 illustrates the resulting compression-relaxation isotherms. The hydrophobic WEs required five consecutive compression-relaxation cycles to achieve the final organisation. The WE layers possess several properties in common: they reached very small molecular areas and tolerated high surface pressures during compression, the compressibility of the WE layers decreased gradually during the cycles as indicated by the increased steepness of the isotherms (inset in Figure 13), the lift off area of the isotherms shifted to smaller molecular areas, and, finally, the isotherms exhibited large hysteresis by relaxation as the isotherms suggest. The liquid state WEs, AO and LO, possessed higher compressibilities than the six other WEs and showed less hysteresis at high surface pressures, possibly due to higher fluidity of these layers. The evaporation retardant BO, BP, BLN and BLNN behaved very similarly when compared

to each other. The compression-relaxation cycling of the solid state behenyl laurate (BL) resulted in an extraordinary spike-like isotherm, suggesting close-to-zero compressibility and poor spreading.

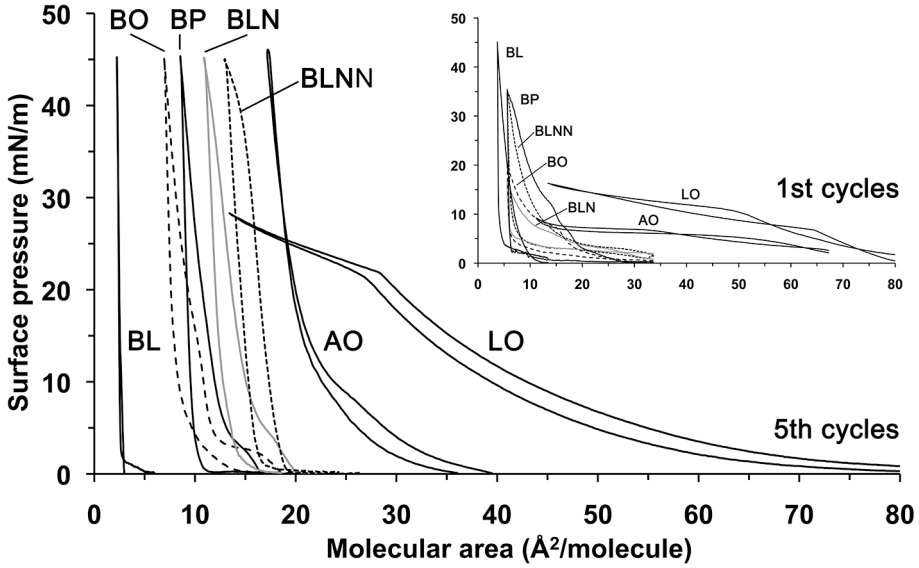

Figure 13. Compression-relaxation isotherms for selected WEs after five cycles at 35 °C. Inset illustrates the first cycles for each WE.
AO, arachidyl oleate; BL, behenyl laurate; BLN, behenyl linoleate; BLNN, behenyl linolenate; BO, behenyl oleate; BP, behenyl palmitoleate; LO, lauryl oleate.

6. DISCUSSION

6.1 Lipid composition of tear fluid

In study I, we investigated the human tear fluid lipid composition mainly using the UPLC-MS technique and complementary methods: TLC and enzymatic assays. We demonstrated that a substantial amount of phospholipids were present in tear fluid, accompanied by CEs, TGs, and most likely WEs. The most common PLs detected in MS analysis were PC and PE, which comprised 88±6% (mol/mol) of the identified lipids. LysoPLs formed a major portion of the PLs, suggesting that phospholipase A2, an abundant tear fluid enzyme, is also highly active (Saari et al. 2001). According to the enzymatic assays and MS profiling of choline-containing lipids, the respective concentrations of 48±14 μM and 22±10 μM are well in line with each other. The findings were well in line with recent mass spectrometric tear fluid lipid composition studies (Ham et al. 2005, Saville et al. 2010, Saville et al. 2011, Dean and Glasgow 2012).

TLC proved to be a somewhat insensitive method for detecting PLs in tear fluid, and we detected only a faint band for SM in our samples. Accordingly, Wollensak and co-workers (Wollensak et al. 1990) were not able to detect PLs in all of their tear samples using high performance TLC. In the non-polar-lipid separation, we detected an abundance of lipid with similar elution distance to CEs. This broad band identified as CEs most likely also contained the WEs (Wollensak et al. 1990), for which we did not possess a reference substance at that time. In line with the apparent abundance of CEs detected in TLC separation, we were able to quantify total cholesterol with an enzymatic lipid assay. We approximated that the concentration of total cholesterol was equal to the concentration of CEs in tear fluid because, in meibum, the cholesterol is mainly in CEs (Chen et al. 2010). The total amount of cholesterol relative to the amount of choline-containing lipid was 40±27%. In addition to TGs, no other non-polar lipids were detected in our MS analysis. Based on MS analysis and enzymatic lipid assays, the amount of TGs relative to choline-containing lipids were 8±5% and 22±6%, respectively. These values are well in line with each other considering the differing analysis techniques. In TLC, faint bands were detected for TGs. Altogether, it needs to be remembered that this is the lipid composition of total aqueous tears, and therefore, the TFLL lipid composition may differ from the one presented here.

The olive-oil-spreading experiments were performed to emphasise on a macroscopic scale the potential function of PLs in TFLL. The contact angles (Figures 8 and 9) on an eggPC-monolayer-coated mica surface showed considerably lower values compared to the blank hydrophilic mica surface representing an air-water interface. On an ocular surface, this would mean that without the polar PL interface, the TFLL would spread inadequately after a blink and would also form a more unstable lipid layer, possibly causing rapid break-up of the tear film.

There are two main findings in this study. (*i*) PLs are abundant in tear fluid, and therefore, the TFLL and meibum lipid composition seem to differ. If assumed that all the polar lipids (PC, PE, ceramide, SM, and PS) detected in MS are located at the air-tear interface, this amount of lipid (28 μM corresponding to 0.28 nmol) would result as a

mean molecular area of approximately 130 $Å^2$/molecule with tear film volume of 10 μL (Mishima 1965) and ocular surface area of 2.2 cm^2 (Tsubota and Nakamori 1995). This molecular area is approximately the lift-off area measured for eggPC monolayers and therefore indicates that, in theory, a monolayer could be formed at the air-tear interface with the aforementioned amount of polar lipids. (*ii*) Such monolayer is possibly needed to aid the organisation of the accompanying non-polar lipids at the air-water interface. The study demonstrates that non-polar lipids, when present in large amounts, spread inefficiently at the air-water interface, and therefore, PLs may be necessary in aiding the spreading of the lipid layer. However, our model, due to the simplified nature of the experiment, gives a very crude description of the phenomenon.

In addition, the origin of the PLs needs to be considered. They may originate from the conjunctival and/or corneal epithelial cells (Butovich 2008); however, no data supporting this theory have been presented.

Finally, it has to be emphasised that based on the lipid composition, we cannot determine the exact location of the polar lipids. In addition to the potential function as a spreading-aid of TFLL, PLs may also be located in the aqueous phase as aggregates such as micelles and liposomes, but they may also be bound to proteins such as lipocalin (Dean and Glasgow 2012). Molecular level functional studies, such as the ones of Kulovesi et al. (2010, 2012), are needed to investigate the impact of compositional changes on the structure and function of TFLL-like lipid layers. Such studies may provide implications of what the ratio could be between lipids in such layers *in vivo,* and finally, what the main function of the TFLL may be. Therefore, studying the impact of lipid composition on the macroscopic properties of lipid layers, such as the potential retardation of evaporation, is equally important.

6.2 Retardation of evaporation

We studied the evaporation-retarding effect of certain selected lipid species of TFLL and their mixtures, and we aimed to show the chemical and physical properties that generate an evaporation-retardant lipid layer. The custom-built system used in these studies produced repeatable results, considering that the system was not isolated from the changing humidity conditions of the lab. However, a constant flow of dried air through the cabinet diminished the effect of the changing humidity conditions. Building an apparatus isolated from the surrounding atmosphere would have guaranteed better repeatability of the results but would have impaired the usability of the device.

6.2.1 Retardation of evaporation by TFLL-like layers

In study II, we investigated the evaporation-retarding effect of TFLL-like lipid layers. The original composition of the lipid layer was selected based on the study I and further adjusted during the study. Additionally, selected pure lipid monolayers, namely eggPC and BO, were investigated to better understand their function in the multi-component mixtures.

First, we wanted to demonstrate that a thick layer of oil (~180 μm) can be employed to retard evaporation from the air-water interface. The decrease of 54%±12% in the evaporation rate suggests that using such layers as evaporation retardants is a somewhat ineffective method because similar efficiency is achieved by specific 5-10 nm thick monolayers, such as BAl.

A simple monolayer of eggPC, a mixture of saturated and unsaturated PCs, did not retard evaporation. This is most likely due to the larger cross-sectional area of PLs, as well as the larger intra-lipid-layer free volume, than long-chain alcohols or long-chain fatty acids.

We studied behenyl oleate layers because certain WEs are known to retard evaporation (Rosano and La Mer 1956, Samuels et al. 2008, Borchman et al. 2009). Due to the relatively hydrophobic nature of behenyl oleate, it was not expected to form a homogeneous monolayer at the air-water interface. The heterogeneous spreading of behenyl oleate is observable by visual inspection. The aggregates spread slowly in near-physiologic temperature, but they do not spread completely. Behenyl oleate at a molecular area of <50 $Å^2$ resulted in a surface pressure of ~4 mN, indicating poor surface activity. Mixtures of PC and BO 1:9 retained the ability to retard evaporation, but the effect was lost when mixed with larger amounts of PC (4:6 and 9:1). The 1:9 PC/BO expectedly exhibited increased surface activity, and the spreading seemed somewhat faster and more homogenous than with pure BO. Possibly, the more effective and homogeneous PC-aided spreading of WE compensates the subtle increase in the fluidity of the layer, and therefore, the evaporation-retarding effect is maintained.

We selected a mixture consisting of 4:2:2:2 PC/CO/TG/BO as a starting composition for the multi-component mixtures. This mixture was an approximation based on the current knowledge of tear fluid lipid composition (study I), meibum composition, and the behaviour of similar monolayers (Kulovesi et al. 2010, 2012). Because this composition did not demonstrate retardation of evaporation, we increased the proportion of non-polar lipids. However, 1:3:3:3 and 1:1:1:7 PC/CE/TG/BO compositions did not retard evaporation either. The non-existent evaporation-retarding effect of the four-component mixtures may be explained by the loose organisation of the lipid layer, as shown previously for similar lipid layers (Kulovesi et al. 2010, 2012).

This hypothesis was in line with the BAM images (Figure 11), which clearly illustrated the differences in the interfacial organisation among the 1:9 PC/BO, 4:2:2:2, 1:3:3:3, and 1:1:1:7 PC/CE/TG/BO. The evaporation-retardant 1:9 PC/BO exhibited a more condensed phase than the four-component lipid layers. This finding suggests that the network of van der Waals interactions required for evaporation retardation does not form between the lipid hydrocarbon chains in complex lipid mixtures i.e., the complex lipid layers are heterogeneous mixtures of disordered and ordered phases.

6.2.2 Retardation of evaporation by wax ester layers

In study III, the WEs were investigated in more detail because BO proved to be an effective evaporation retardant in study II. The WEs were selected as close as possible according to those found in meibum. Our aim was to investigate whether all of these WEs retard evaporation or whether the retardation is only a property of specific WEs.

The MPs of WEs were determined because these data were only partially available from the literature (Iyengar and Schlenk 1969). Based on the MPs, the WEs were grouped into three melting-point categories: MPs well below physiological temperature, close to the physiological temperature, and clearly above physiological temperature (see Table 2 for the categories).

We measured the evaporation rates at a near-physiologic temperature of 35 °C and discovered that only four WEs retarded evaporation (Figure 10). BP, BLN, and BLNN, in addition to the BO decreased evaporation rates by 20-40%. These four WEs melted within 2 °C of the physiological temperature. Overall, visual inspection of the WE layers suggested that the high-MP WEs formed raft-like aggregates at the air-water interface, whereas low-MP WEs exhibited more homogenous spreading.

Because the retardation of evaporation by WEs was apparently related to the MP, we measured the evaporation rates through the four retardant WEs at 30 °C and 41 °C to determine whether these lipids retard evaporation when they are in a solid or in a liquid state. At 30 °C, BLN and BLNN decreased evaporation by ~50%, whereas BP and BO retarded evaporation only by 5-10%. At 41 °C, the decrease in evaporation was only 2-4% (Figure 10).

To further confirm our theory, we measured the evaporation-retarding effect of AO at 30 °C and 41 °C in addition to 35 °C. Based on the MP of 33 °C, AO should retard evaporation only at 30 °C. This turned out to be true: the decrease in evaporation was 16±1%, whereas no retardation was observed at 35 °C or at 41 °C.

The spreading of WE species was observed using BAM (Figure 12). Long-chain saturated LL formed thick three-dimensional aggregates at the interface, whereas the short-chain LO spread more homogenously. The similar extent of aggregation and analogous surface pressures of BO, BLNN, and BLN imply that these WE layers were in the same phase. BP also spread rapidly when applied to the interface, but the layer also appeared largely layered and aggregated. The somewhat larger areas of grey shade and the stagnant appearance of BP also reminds of a phase that is condensed or gel-like compared to the more fluid BO, BLN, and BLNN layers, which may explain the more efficient retardation of evaporation. For reference, the left-hand side panel in Figure 12 shows a homogenously spread BAl layer. The grey shade, presented clearly in the high-exposure image (lower image), illustrates a monolayer entirely in condensed phase.

The evaporation experiments and the BAM images suggested that the differences in the evaporation-retarding effects of WEs were due to physicochemical properties of WEs when they are close to their melting phase transition. In their solid state, large areas of the interface are not covered by lipid, and the lipid forms three-dimensional aggregates at the air-water interface. Alternatively, in very fluid-like layers, the extensive thermal motion of the lipid molecules accumulates a large free-volume within the lipid membrane therefore allowing the water molecules to diffuse through the WE layer (Sane et al.

2009). Close to their melting phase transition, WEs form a condensed-like phase that retards evaporation. The differing efficiency in retardation of evaporation between specific WEs possibly arises from the MP–dependent interplay between the spreading rate of the lipid and the level of condensation of the layer.

6.3 Surface active properties of wax esters

In addition, we studied the surface active properties of the somewhat hydrophobic WEs at the air-water interface under consecutive compression-relaxation cycles, to assess if such lipids could act as surfactants in dynamic environment. The evaporation-retardant effect strongly suggests that the WEs form an organised structure at the air-water interface. However, we investigated how the WEs compared to more traditional surfactants, such as PLs in a dynamic environment.

The isotherms illustrate that the differing WE layers share similar behaviour under compression (Figure 13). The transfer of the lift-off area between 1st cycles and 5th cycles is explained by increased aggregation, i.e., WEs are forced out of the interface into three-dimensional aggregates. Compression causes the WE layer to aggregate increasingly, and because of the hydrophobic nature of WEs, it is energetically more favourable for the aggregated molecules not to spread to the interface on relaxation. This impaired re-spreading results in large hysteresis apparent in the isotherms. The transfer of the molecules into the bulk phase shows also as a decrease in compressibility as indicated by the steepening isotherms. However, the high surface pressures and the tolerance against collapsing suggest that at the air-water interface, WEs arrange into an organised lateral structure. In relation to the *in vivo* TFLL, it has to be noted that the lid-sweeping motion on the ocular surface is very rapid. For hydrophobic lipids such as WEs, the prevailing conditions on the ocular surface would further promote aggregation.

Among the seven investigated WEs, the behaviour of liquid state LO and AO resembled that of a surfactant: they were more compressible and showed less hysteresis than the other WEs, especially at the high surface pressures. In contrast, the cycling of solid state BL resulted in a spike-like isotherm profile. This is explained by the impaired spreading and close-to-zero compressibility of the solid-state WE. The isotherms of the evaporation-retardant WEs expectedly located between the solid state BL and liquid AO. Overall, the Langmuir film experiments unveiled the poor compression-expansion behaviour of the WE layers relative to that of PLs. Fluid WE layer (LO and AO) showed surfactant-like behaviour, whereas WE close to the phase transition and in solid phase exhibited increasing tendency to aggregation.

In conclusion, only specific WEs retarded evaporation at physiological temperatures. The ability to retard evaporation is dependent on the physical properties of the WEs at a given temperature. The evaporation-retarding effect may be explained by the formation of a specific condensed-like phase of the WE layer, which exists at the proximity of the melting phase transition. Under consecutive compression-relaxation cycles the build-up of aggregated WE structures continues until a pressure-tolerant WE layer is formed. Despite the high surface pressure tolerance, WEs spread very slowly to the interface,

prefer aggregation over homogenous spreading, are incompressible, and create lipid layers that are unstable in a dynamic environment. In relation to TFLL, under rapid compression-relaxation cycling induced by the lids, the WEs would be extensively aggregated. In addition, considering the time-scale of the inter-blink period, virtually no re-spreading would occur.

7. SUMMARY AND CONCLUSIONS

In this thesis project, we first investigated the lipid composition of human tear fluid by using modern mass spectrometric techniques, concentrating mainly on the PL content of the tear fluid. As we expected, the tear fluid contained a considerable proportion of PLs, and we illustrated the plausible spreading-aiding function of these amphipathic lipids. However, a quantitative lipid composition could not be obtained because no comprehensive method was available for both polar and non-polar lipids. Based on the lipid composition and an assumption that most of the tear film lipids are located at the air-tear interface, we created TFLL-like compositions as an *in vitro* model of the TFLL. We investigated the evaporation-retarding effect of these TFLL-like compositions, and we discovered that most of the compositions, surprisingly, did not retard evaporation. Instead, pure WEs, an abundant lipid species in meibum, was shown to effectively retard evaporation, provided the layer was in a specific condensed-like temperature-dependent phase. The hydrophobic WEs were prone to aggregation, particularly in evaporation-retarding conditions, and were therefore poor surfactants in dynamic environment. Mixing PLs with the WEs aided the spreading of the layer, but the evaporation-retarding effect decreased rapidly with the increased fluidity induced by the lipid layer. In conclusion, the fluidic, rapidly spreading, lipid layers typically retard evaporation poorly; whereas the poorly spreading and aggregation-prone WEs are effective evaporation retardants provided the layer is in a defined phase.

The results suggest that qualitative or quantitative changes in the TFLL composition, such as changes in the relative proportions of the lipid classes, variations in the degree of saturation, or increased branching of the lipid chains may alter the properties, such as the phase transition temperature, of the TFLL. Such changes may be due to defective synthesis of the lipids or to a decrease in the amount of the lipid-anti-oxidative agents in the tear film. An insufficient amount of PLs potentially affects the spreading of the non-polar lipids and impairs the formation of a uniform lipid layer. Additionally, in analogy to WEs, an increase in the phase transition temperature may increase the solidity of meibum, and therefore result in aggregation and, therefore, poor spreading of the lipids at the air-water interface. In contrast, a decrease in the phase transition temperature could result in increased fluidity of the layer, and thus, increased evaporation of the aqueous tears. Altogether, such variations would hinder the formation of an evaporation-retardant TFLL, result in hyperosmolarity due to increased evaporation, and finally lead to dry eye symptoms. However, further studies are needed to investigate whether such behaviour is also observed with meibum.

Certain eye drop solutions targeted for dry eye treatment contain lipids. Very often, the lipid composition of the solution is not revealed, but they typically contain mineral oils accompanied by a variety of other lipids such as phospholipids. Mineral oil, a mixture of differing alkanes often also employed in various cosmetic products could retard evaporation in large amounts, such as the thick layer of olive oil illustrated in our studies. However, application of such large volumes of lipid on the ocular surface does not seem practical. The application of phospholipids also does not increase the evaporation-retarding effect of the TFLL. Therefore, the modern lipid-containing eye drops most likely do not increase the evaporation-retarding effect of the lipid layer, but

moreover provide anti-inflammatory or lubricative effects. Lipid-containing eye drop solutions, which would actually restore the TFLL function, represent an important target for research and development. However, the evaporation-retarding lipids may be challenging for this purpose because they form very stiff non-elastic films, which are poorly suitable for the dynamic environments of the ocular surface.

In conclusion, although the WEs comprise a major part of the meibum, it also contains as much as 70% of CEs and other lipids. Therefore, the underlying mechanism of evaporation-retarding TFLL has been only partly elucidated. The results suggest that WEs constitute an important component of the potent evaporation-retarding TFLL, and PLs play a role as a spreading-aid of such aggregation-prone non-polar lipids, but possibly at lower proportions than originally hypothesised. The next piece in this puzzle is the role of the abundant tear fluid CEs – one major research topic of our future studies.

ACKNOWLEDGEMENTS

This thesis project was carried out in the Helsinki Eye Lab at the Department of Ophthalmology, University of Helsinki, and in the Public Health Genomics Research Unit, National Institute for Health and Welfare, during the years 2009-2013. I wish to thank the head of the Department of Ophthalmology Adjunct Professor Erna Kentala, and Professors Tero Kivelä and Timo Tervo, and the head of the Public Health Genomics Research Unit Adjunct Professor Anu Jalanko for providing research facilities.

I wish to express my deepest gratitude and thanks to my supervisors Adjunct Professors Juha Holopainen and Susanne Wiedmer. Juha is one of the most inspirational scientists I have met and his infectious enthusiasm has kept me going. Additionally, the never-ending patience and the sense of humour are admirable, not to mention the high level of knowledge, dedication, and the professional insight into science. It has been a privilege to work with Susanne since my master thesis studies, and her efficiency and dedication are something that I have been trying to adopt. Since the Kumpula years, her lab door has been open, and I'm grateful for all the help, patience, and guidance during the past years.

I also wish to thank the reviewers of this thesis, Professor Ben Glasgow and Professor J. Peter Slotte, for the efficient review process and the valuable comments and suggestions.

I have been honoured to work with number of collaborators during this project. I wish to thank Adjunct Professor Matti Jauhiainen for all the collaboration, help, and, particularly, for the practical arrangements at the Public Health Genomics Research Unit. Additionally, it has been a delight to collaborate with Professors Ilpo Vattulainen and Matej Oresic, Artturi Koivuniemi PhD, Jelena Telenius PhD, Matti Javanainen MSc, and Tuulikki Seppänen-Laakso PhD. I warmly thank all the personnel and the researchers in the Department of Ophthalmology and the Public Health Genomics Research Unit.

It has been a privilege to work with talented colleagues in the Helsinki Eye Lab, Alexandra Robciuc MSc, Pipsa Kulovesi MSc, and Riku Paananen BEng. This group created an inspirational and relaxed working atmosphere, and it has been a delight to be part of the group. I would also like to specially thank Alexandra. She always found the time for "peer-group therapy", when things were not going as planned. I really enjoyed those discussions on science and, particularly, life in general. Additionally, many thanks for the endless help in the lab.

Thanks also go to the bike-riding mates of Seinäjoki Freeride. You have been like brothers to me helping me live the other type of dream outside of science. I also want thank my PS chemist colleagues for the friendship all the way from the AnLab years.

Finally, I want to express my deepest gratitude to my parents Seija and Jorma and my brother Juha. You have been terrific role models, formed a safe and warm family to grow in, and have taught the right values in life. Thank you for the unconditional love and support over the years.

The Academy of Finland, the Eye and Tissue Bank Foundation, The Finnish Eye Foundation, the Nissi Foundation, and the Sigrid Juselius Foundation funded the study.

Helsinki, January 10th 2014

Antti Rantamäki

REFERENCES

Albers JJ, Wolfbauer G, Cheung MC, Day JR, Ching AF, Lok S, and Tu AY (1995). Functional expression of human and mouse plasma phospholipid transfer protein: effect of recombinant and plasma PLTP on HDL subspecies. Biochim. Biophys. Acta 1258: 27-34.

Arciniega JC, Uchiyama E, and Butovich IA (2013). Disruption and destabilization of meibomian lipid films caused by increasing amounts of ceramides and cholesterol. Invest. Ophthalmol. Vis. Sci. 54: 1352-1360.

Argueso P, Spurr-Michaud S, Russo CL, Tisdale A, and Gipson IK (2003). MUC16 mucin is expressed by the human ocular surface epithelia and carries the H185 carbohydrate epitope. Invest. Ophthalmol. Vis. Sci. 44: 2487-2495.

Arnold RR, Cole MF, and McGhee JR (1977). A bactericidal effect for human lactoferrin. Science 197: 263-265.

Ban Y, Dota A, Cooper LJ, Fullwood NJ, Nakamura T, Tsuzuki M, Mochida C, and Kinoshita S (2003). Tight junction-related protein expression and distribution in human corneal epithelium. Exp. Eye Res. 76: 663-669.

Baoukina S, Monticelli L, Amrein M, and Tieleman DP (2007). The molecular mechanism of monolayer-bilayer transformations of lung surfactant from molecular dynamics simulations. Biophys. J. 93: 3775-3782.

Baoukina S, Monticelli L, Risselada HJ, Marrink SJ, and Tieleman DP (2008). The molecular mechanism of lipid monolayer collapse. Proc. Natl. Acad. Sci. U. S. A. 105: 10803-10808.

Barnes GT (2008). The potential for monolayers to reduce the evaporation of water from large water storages. Agric. Water Manage. 95: 339-353.

Battat L, Macri A, Dursun D, and Pflugfelder SC (2001). Effects of laser in situ keratomileusis on tear production, clearance, and the ocular surface. Ophthalmology 108: 1230-1235.

Beuerman RW and Pedroza L (1996). Ultrastructure of the human cornea. Microsc. Res. Tech. 33: 320-335.

Blalock TD, Spurr-Michaud SJ, Tisdale AS, Heimer SR, Gilmore MS, Ramesh V, and Gipson IK (2007). Functions of MUC16 in corneal epithelial cells. Invest. Ophthalmol. Vis. Sci. 48: 4509-4518.

Borchman D, Foulks GN, Yappert MC, Mathews J, Leake K, and Bell J (2009). Factors affecting evaporation rates of tear film components measured in vitro. Eye Contact Lens 35: 32-37.

Brauer L, Johl M, Borgermann J, Pleyer U, Tsokos M, and Paulsen FP (2007). Detection and localization of the hydrophobic surfactant proteins B and C in human tear fluid and the human lacrimal system. Curr. Eye Res. 32: 931-938.

Brauer L, Kindler C, Jager K, Sel S, Nolle B, Pleyer U, Ochs M, and Paulsen FP (2007). Detection of surfactant proteins A and D in human tear fluid and the human lacrimal system. Invest. Ophthalmol. Vis. Sci. 48: 3945-3953.

Braun RJ and Fitt AD (2003). Modelling drainage of the precorneal tear film after a blink. Mathematical Medicine and Biology 20: 1-28.

Bron AJ and Tiffany JM (2004). The contribution of meibomian disease to dry eye. Ocul. Surf. 2: 149-165.

Bron AJ, Tiffany JM, Gouveia SM, Yokoi N, and Voon LW (2004). Functional aspects of the tear film lipid layer. Exp. Eye Res. 78: 347-360.

Butovich IA (2013). Tear film lipids. Exp. Eye Res. 117: 4-27.

Butovich IA (2011). Lipidomics of human Meibomian gland secretions: Chemistry, biophysics, and physiological role of Meibomian lipids. Prog. Lipid Res. 50: 278-301.

Butovich IA (2010). Fatty acid composition of cholesteryl esters of human meibomian gland secretions. Steroids 75: 726-733.

Butovich IA (2009). Lipidomic analysis of human meibum using HPLC-MSn. Methods Mol. Biol. 579: 221-246.

Butovich IA (2008). On the lipid composition of human meibum and tears: comparative analysis of nonpolar lipids. Invest. Ophthalmol. Vis. Sci. 49: 3779-3789.

Butovich IA, Arciniega JC, Lu H, and Molai M (2012). Evaluation and quantitation of intact wax esters of human meibum by gas-liquid chromatography-ion trap mass spectrometry. Invest. Ophthalmol. Vis. Sci. 53: 3766-3781.

Butovich IA, Millar TJ, and Ham BM (2008). Understanding and analyzing meibomian lipids--a review. Curr. Eye Res. 33: 405-420.

Butovich IA, Uchiyama E, Di Pascuale MA, and McCulley JP (2007). Liquid chromatography-mass spectrometric analysis of lipids present in human meibomian gland secretions. Lipids 42: 765-776.

Butovich IA, Uchiyama E, and McCulley JP (2007). Lipids of human meibum: mass-spectrometric analysis and structural elucidation. J. Lipid Res. 48: 2220-2235.

Cenedella RJ and Fleschner CR (1990). Kinetics of corneal epithelium turnover in vivo. Studies of lovastatin. Invest. Ophthalmol. Vis. Sci. 31: 1957-1962.

Cerretani CF, Ho NH, and Radke CJ (2013). Water-evaporation reduction by duplex films: application to the human tear film. Adv. Colloid Interface Sci. 197-198: 33-57.

Chen J, Green-Church KB, and Nichols KK (2010). Shotgun lipidomic analysis of human meibomian gland secretions with electrospray ionization tandem mass spectrometry. Invest. Ophthalmol. Vis. Sci. 51: 6220-6231.

Craig JP, Singh I, Tomlinson A, Morgan PB, and Efron N (2000). The role of tear physiology in ocular surface temperature. Eye 14: 635-641.

Craig JP and Tomlinson A (1997). Importance of the lipid layer in human tear film stability and evaporation. Optom. Vis. Sci. 74: 8-13.

Dartt DA (2009). Neural regulation of lacrimal gland secretory processes: relevance in dry eye diseases. Prog. Retin. Eye Res. 28: 155-177.

de Souza GA, Godoy LM, and Mann M (2006). Identification of 491 proteins in the tear fluid proteome reveals a large number of proteases and protease inhibitors. Genome Biol. 7: R72.

Dean AW and Glasgow BJ (2012). Mass spectrometric identification of phospholipids in human tears and tear lipocalin. Invest. Ophthalmol. Vis. Sci. 53: 1773-1782.

Doughty MJ and Zaman ML (2000). Human corneal thickness and its impact on intraocular pressure measures: a review and meta-analysis approach. Surv. Ophthalmol. 44: 367-408.

Ehlers N (1970). Some comparative studies on the mammalian corneal epithelium. Acta Ophthalmol. (Copenh) 48: 821-828.

Ehlers N and Hjortdal J (2006). The Cornea: Epithelium and Stroma. Advances in Organ Biology. Elsevier, pp. 83-111

Ehlers N and Hjortdal J (2004). Corneal thickness: measurement and implications. Exp. Eye Res. 78: 543-548.

Farnaud S and Evans RW (2003). Lactoferrin--a multifunctional protein with antimicrobial properties. Mol. Immunol. 40: 395-405.

Fini ME and Stramer BM (2005). How the cornea heals: cornea-specific repair mechanisms affecting surgical outcomes. Cornea 24: S2-S11.

Fleming A (1922). On a remarkable bacteriolytic element found in tissues and secretions. Proceedings of the Royal Society of London. Series B, Containing Papers of a Biological Character 93: 306-317.

Folch J, Lees M, and Sloane Stanley GH (1957). A simple method for the isolation and purification of total lipides from animal tissues. J. Biol. Chem. 226: 497-509.

Foulks GN and Bron AJ (2003). Meibomian gland dysfunction: a clinical scheme for description, diagnosis, classification, and grading. Ocul. Surf. 1: 107-126.

Gasymov OK, Abduragimov AR, Prasher P, Yusifov TN, and Glasgow BJ (2005). Tear lipocalin: evidence for a scavenging function to remove lipids from the human corneal surface. Invest. Ophthalmol. Vis. Sci. 46: 3589-3596.

Gharib SA, Vaisar T, Aitken ML, Park DR, Heinecke JW, and Fu X (2009). Mapping the lung proteome in cystic fibrosis. J. Proteome Res. 8: 3020-3028.

Gilbard JP and Farris RL (1983). Ocular surface drying and tear film osmolarity in thyroid eye disease. Acta Ophthalmol. (Copenh) 61: 108-116.

Gipson IK, Spurr-Michaud SJ, and Tisdale AS (1987). Anchoring fibrils form a complex network in human and rabbit cornea. Invest. Ophthalmol. Vis. Sci. 28: 212-220.

Glasgow BJ, Abduragimov AR, Farahbakhsh ZT, Faull KF, and Hubbell WL (1995). Tear lipocalins bind a broad array of lipid ligands. Curr. Eye Res. 14: 363-372.

Glasgow BJ, Gasymov OK, Abduragimov AR, Engle JJ, and Casey RC (2010). Tear lipocalin captures exogenous lipid from abnormal corneal surfaces. Invest. Ophthalmol. Vis. Sci. 51: 1981-1987.

Glasgow BJ, Marshall G, Gasymov OK, Abduragimov AR, Yusifov TN, and Knobler CM (1999). Tear lipocalins: potential lipid scavengers for the corneal surface. Invest. Ophthalmol. Vis. Sci. 40: 3100-3107.

Goto E and Tseng SC (2003). Kinetic analysis of tear interference images in aqueous tear deficiency dry eye before and after punctal occlusion. Invest. Ophthalmol. Vis. Sci. 44: 1897-1905.

Ham BM, Jacob JT, and Cole RB (2005). MALDI-TOF MS of phosphorylated lipids in biological fluids using immobilized metal affinity chromatography and a solid ionic crystal matrix. Anal. Chem. 77: 4439-4447.

Hanna C, Bicknell DS, and O'Brien JE (1961). Cell turnover in the adult human eye. Arch. Ophthalmol. 65: 695-698.

Heath P (1948). Ocular Lymphomas. Trans. Am. Ophthalmol. Soc. 46: 385-398.

Heigle TJ and Pflugfelder SC (1996). Aqueous tear production in patients with neurotrophic keratitis. Cornea 15: 135-138.

Henry DJ, Dewan VI, Prime EL, Qiao GG, Solomon DH, and Yarovsky I (2010). Monolayer structure and evaporation resistance: a molecular dynamics study of octadecanol on water. J Phys Chem B 114: 3869-3878.

Herok GH, Mudgil P, and Millar TJ (2009). The effect of Meibomian lipids and tear proteins on evaporation rate under controlled in vitro conditions. Curr. Eye Res. 34: 589-597.

Holly FJ (1973). Formation and rupture of the tear film. Exp. Eye Res. 15: 515-525.

Holopainen JM, Brockman HL, Brown RE, and Kinnunen PK (2001). Interfacial interactions of ceramide with dimyristoylphosphatidylcholine: impact of the N-acyl chain. Biophys. J. 80: 765-775.

Hsu JK, Cavanagh HD, Jester JV, Ma L, and Petroll WM (1999). Changes in corneal endothelial apical junctional protein organization after corneal cold storage. Cornea 18: 712-720.

Ihanamaki T, Pelliniemi LJ, and Vuorio E (2004). Collagens and collagen-related matrix components in the human and mouse eye. Prog. Retin. Eye Res. 23: 403-434.

Inatomi T, Spurr-Michaud S, Tisdale AS, and Gipson IK (1995). Human corneal and conjunctival epithelia express MUC1 mucin. Invest. Ophthalmol. Vis. Sci. 36: 1818-1827.

Inatomi T, Spurr-Michaud S, Tisdale AS, Zhan Q, Feldman ST, and Gipson IK (1996). Expression of secretory mucin genes by human conjunctival epithelia. Invest. Ophthalmol. Vis. Sci. 37: 1684-1692.

Iwata S, Lemp MA, Holly FJ, and Dohlman CH (1969). Evaporation rate of water from the precorneal tear film and cornea in the rabbit. Invest. Ophthalmol. 8: 613-619.

Iyengar BT and Schlenk H (1969). Melting points of synthetic wax esters. Lipids 4: 28-30.

James DG, Anderson R, Langley D, and Ainslie D (1964). Ocular Sarcoidosis. Br. J. Ophthalmol. 48: 461-470.

Janmey PA and Schliwa M (2008). Rheology. Curr. Biol. 18: R639-R641.

Jauhiainen M, Setälä NL, Ehnholm C, Metso J, Tervo TM, Eriksson O, and Holopainen JM (2005). Phospholipid transfer protein is present in human tear fluid. Biochemistry 44: 8111-8116.

Jester JV, Petroll WM, and Cavanagh HD (1999). Corneal stromal wound healing in refractive surgery: the role of myofibroblasts. Prog. Retin. Eye Res. 18: 311-356.

Jiang XC, D'Armiento J, Mallampalli RK, Mar J, Yan SF, and Lin M (1998). Expression of plasma phospholipid transfer protein mRNA in normal and emphysematous lungs and regulation by hypoxia. J. Biol. Chem. 273: 15714-15718.

Johansson J, Curstedt T, and Robertson B (1994). The proteins of the surfactant system. European Respiratory Journal 7: 372-391.

Kardon R, Price RE, Julian J, Lagow E, Tseng SC, Gendler SJ, and Carson DD (1999). Bacterial conjunctivitis in Muc1 null mice. Invest. Ophthalmol. Vis. Sci. 40: 1328-1335.

Karson CN, Burns RS, LeWitt PA, Foster NL, and Newman RP (1984). Blink rates and disorders of movement. Neurology 34: 677-678.

Karttunen M, Haataja MP, Saily M, Vattulainen I, and Holopainen JM (2009). Lipid domain morphologies in phosphatidylcholine-ceramide monolayers. Langmuir 25: 4595-4600.

King-Smith PE, Fink BA, Hill RM, Koelling KW, and Tiffany JM (2004). The thickness of the tear film. Curr. Eye Res. 29: 357-368.

King-Smith PE, Fink BA, Nichols JJ, Nichols KK, Braun RJ, and McFadden GB (2009). The contribution of lipid layer movement to tear film thinning and breakup. Invest. Ophthalmol. Vis. Sci. 50: 2747-2756.

King-Smith PE, Hinel EA, and Nichols JJ (2010). Application of a novel interferometric method to investigate the relation between lipid layer thickness and tear film thinning. Invest. Ophthalmol. Vis. Sci. 51: 2418-2423.

Komai Y and Ushiki T (1991). The three-dimensional organization of collagen fibrils in the human cornea and sclera. Invest. Ophthalmol. Vis. Sci. 32: 2244-2258.

Kulovesi P, Telenius J, Koivuniemi A, Brezesinski G, Rantamäki A, Viitala T, Puukilainen E, Ritala M, Wiedmer SK, Vattulainen I, and Holopainen JM (2010). Molecular organization of the tear fluid lipid layer. Biophys. J. 99: 2559-2567.

Kulovesi P, Telenius J, Koivuniemi A, Brezesinski G, Vattulainen I, and Holopainen JM (2012). The impact of lipid composition on the stability of the tear fluid lipid layer. Soft Matter 8: 5826-5834.

La Mer VK and Healy TW (1965). Evaporation of Water: Its Retardation by Monolayers: Spreading a monomolecular film on the surface is a tested and economical means of reducing water loss. Science 148: 36-42.

Lam SM, Tong L, Yong SS, Li B, Chaurasia SS, Shui G, and Wenk MR (2011). Meibum lipid composition in Asians with dry eye disease. PLoS One 6: e24339.

Lehrer RI, Xu G, Abduragimov A, Dinh NN, Qu XD, Martin D, and Glasgow BJ (1998). Lipophilin, a novel heterodimeric protein of human tears. FEBS Lett. 432: 163-167.

Leiske DL, Raju SR, Ketelson HA, Millar TJ, and Fuller GG (2010). The interfacial viscoelastic properties and structures of human and animal Meibomian lipids. Exp. Eye Res. 90: 598-604.

Lemp MA, Baudouin C, Baum J, Dogru M, Foulks GN, Kinoshita S, Laibson P, McCulley J, Murube J, Pflugfelder SC, Rolando M, and Toda I (2007). The definition and classification of dry eye disease: report of the Definition and Classification Subcommittee of the International Dry Eye WorkShop (2007). Ocul. Surf. 5: 75-92.

Luisi PL, de Souza TP, and Stano P (2008). Vesicle behavior: in search of explanations. J Phys Chem B 112: 14655-14664.

Mantelli F and Argueso P (2008). Functions of ocular surface mucins in health and disease. Curr. Opin. Allergy Clin. Immunol. 8: 477-483.

Marfurt CF and Ellis LC (1993). Immunohistochemical localization of tyrosine hydroxylase in corneal nerves. J. Comp. Neurol. 336: 517-531.

Marfurt CF, Jones MA, and Thrasher K (1998). Parasympathetic innervation of the rat cornea. Exp. Eye Res. 66: 437-448.

Marshall GE, Konstas AG, and Lee WR (1993). Collagens in ocular tissues. Br. J. Ophthalmol. 77: 515-524.

Mathers WD, Lane JA, and Zimmerman MB (1996). Tear film changes associated with normal aging. Cornea 15: 229-234.

McCulley JP and Dougherty JM (1985). Blepharitis associated with acne rosacea and seborrheic dermatitis. Int. Ophthalmol. Clin. 25: 159-172.

McCulley JP and Shine W (1997). A compositional based model for the tear film lipid layer. Trans. Am. Ophthalmol. Soc. 95: 79-88; discussion 88-93.

Merkel D, Rist W, Seither P, Weith A, and Lenter MC (2005). Proteomic study of human bronchoalveolar lavage fluids from smokers with chronic obstructive pulmonary disease by combining surface-enhanced laser desorption/ionization-mass spectrometry profiling with mass spectrometric protein identification. Proteomics 5: 2972-2980.

Millar TJ and King-Smith PE (2012). Analysis of comparison of human meibomian lipid films and mixtures with cholesteryl esters In vitro films using high resolution color microscopy. Invest. Ophthalmol. Vis. Sci. 53: 4710-4719.

Miller KL, Polse KA, and Radke CJ (2002). Black-line formation and the "perched" human tear film. Curr. Eye Res. 25: 155-162.

Mishima S (1965). Some physiological aspects of the precorneal tear film. Archives of Ophthalmology 73: 233-241.

Mishima S, Gasset A, Klyce SD,Jr, and Baum JL (1966). Determination of tear volume and tear flow. Invest. Ophthalmol. 5: 264-276.

Mishima S and Maurice DM (1961). The oily layer of the tear film and evaporation from the corneal surface. Exp. Eye Res. 1: 39-45.

Möhwald H (1990). Phospholipid and phospholipid-protein monolayers at the air/water interface. Annu. Rev. Phys. Chem. 41: 441-476.

Morgan C, DeGroat WC, and Jannetta PJ (1987). Sympathetic innervation of the cornea from the superior cervical ganglion. An HRP study in the cat. J. Auton. Nerv. Syst. 20: 179-183.

Müller LJ, Marfurt CF, Kruse F, and Tervo TM (2003). Corneal nerves: structure, contents and function. Exp. Eye Res. 76: 521-542.

Müller LJ, Pels L, and Vrensen GF (1996). Ultrastructural organization of human corneal nerves. Invest. Ophthalmol. Vis. Sci. 37: 476-488.

Müller LJ, Pels L, and Vrensen GF (1995). Novel aspects of the ultrastructural organization of human corneal keratocytes. Invest. Ophthalmol. Vis. Sci. 36: 2557-2567.

Müller LJ, Vrensen GF, Pels L, Cardozo BN, and Willekens B (1997). Architecture of human corneal nerves. Invest. Ophthalmol. Vis. Sci. 38: 985-994.

Nakamori K, Odawara M, Nakajima T, Mizutani T, and Tsubota K (1997). Blinking is controlled primarily by ocular surface conditions. Am. J. Ophthalmol. 124: 24-30.

Nevalainen TJ, Aho HJ, and Peuravuori H (1994). Secretion of group 2 phospholipase A2 by lacrimal glands. Invest. Ophthalmol. Vis. Sci. 35: 417-421.

Nichols B, Dawson CR, and Togni B (1983). Surface features of the conjunctiva and cornea. Invest. Ophthalmol. Vis. Sci. 24: 570-576.

Nichols JJ, Nichols KK, Puent B, Saracino M, and Mitchell GL (2002). Evaluation of tear film interference patterns and measures of tear break-up time. Optom. Vis. Sci. 79: 363-369.

Nicolaides N, Kaitaranta JK, Rawdah TN, Macy JI, Boswell FM,3rd, and Smith RE (1981). Meibomian gland studies: comparison of steer and human lipids. Invest. Ophthalmol. Vis. Sci. 20: 522-536.

Nicolaides N and Santos EC (1985). The di- and triesters of the lipids of steer and human meibomian glands. Lipids 20: 454-467.

Notter RH, (2000). Lung surfactants. Basic science and clinical applications. Marcel Dekker Inc., New York, NY.

Owens H and Phillips J (2001). Spreading of the tears after a blink: velocity and stabilization time in healthy eyes. Cornea 20: 484-487.

Palakuru JR, Wang J, and Aquavella JV (2007). Effect of blinking on tear dynamics. Invest. Ophthalmol. Vis. Sci. 48: 3032-3037.

Patra M, Salonen E, Terama E, Vattulainen I, Faller R, Lee BW, Holopainen J, and Karttunen M (2006). Under the influence of alcohol: the effect of ethanol and methanol on lipid bilayers. Biophys. J. 90: 1121-1135.

Phillips DC (1967). The Hen Egg-White Lysozyme Molecule. Proceedings of the National Academy of Sciences 57: 483-495.

Pluskal T, Castillo S, Villar-Briones A, and Oresic M (2010). MZmine 2: modular framework for processing, visualizing, and analyzing mass spectrometry-based molecular profile data. BMC Bioinformatics 11: 395.

Pritchard N and Fonn D (1995). Dehydration, lens movement and dryness ratings of hydrogel contact lenses. Ophthalmic Physiol. Opt. 15: 281-286.

Raju SR, Palaniappan CK, Ketelson HA, Davis JW, and Millar TJ (2013). Interfacial dilatational viscoelasticity of human meibomian lipid films. Curr. Eye Res. 38: 817-824.

Rantamäki AH, Telenius J, Koivuniemi A, Vattulainen I, and Holopainen JM (2011). Lessons from the biophysics of interfaces: Lung surfactant and tear fluid. Prog. Retin. Eye Res. 30: 204-215.

Robciuc A, Rantamäki AH, Jauhiainen M, and Holopainen JM (2014). Lipid modifying enzymes in human tear fluid and corneal epithelial stress response. Invest. Ophthalmol. Vis. Sci. 55: 16-24.

Rosano HL and La Mer VK (1956). The Rate of Evaporation of Water through Monolayers of Esters, Acids and Alcohols. J. Phys. Chem. 60: 348-353.

Rosenfeld L, Cerretani C, Leiske DL, Toney MF, Radke CJ, and Fuller GG (2013). Structural and rheological properties of meibomian lipid. Invest. Ophthalmol. Vis. Sci. 54: 2720-2732.

Rosenfeld L and Fuller GG (2012). Consequences of interfacial viscoelasticity on thin film stability. Langmuir 28: 14238-14244.

Rozsa AJ and Beuerman RW (1982). Density and organization of free nerve endings in the corneal epithelium of the rabbit. Pain 14: 105-120.

Rufer F, Schroder A, and Erb C (2005). White-to-white corneal diameter: normal values in healthy humans obtained with the Orbscan II topography system. Cornea 24: 259-261.

Ruskell GL (1974). Ocular fibres of the maxillary nerve in monkeys. J. Anat. 118: 195-203.

Saaren-Seppälä H, Jauhiainen M, Tervo TM, Redl B, Kinnunen PK, and Holopainen JM (2005). Interaction of purified tear lipocalin with lipid membranes. Invest. Ophthalmol. Vis. Sci. 46: 3649-3656.

Saari KM, Aho VV, Paavilainen V, and Nevalainen TJ (2001). Group II PLA2 content of tears in normal subjects. Invest. Ophthalmol. Vis. Sci. 42: 318-320.

Salvetat ML, Zeppieri M, Miani F, Parisi L, Felletti M, and Brusini P (2011). Comparison between laser scanning in vivo confocal microscopy and noncontact specular microscopy in assessing corneal endothelial cell density and central corneal thickness. Cornea 30: 754-759.

Samuels L, Kunst L, and Jetter R (2008). Sealing plant surfaces: cuticular wax formation by epidermal cells. Annu. Rev. Plant. Biol. 59: 683-707.

Sane P, Salonen E, Falck E, Repakova J, Tuomisto F, Holopainen JM, and Vattulainen I (2009). Probing biomembranes with positrons. J Phys Chem B 113: 1810-1812.

Saville JT, Zhao Z, Willcox MD, Ariyavidana MA, Blanksby SJ, and Mitchell TW (2011). Identification of phospholipids in human meibum by nano-electrospray ionisation tandem mass spectrometry. Exp. Eye Res. 92: 238-240.

Saville JT, Zhao Z, Willcox MD, Blanksby SJ, and Mitchell TW (2010). Detection and quantification of tear phospholipids and cholesterol in contact lens deposits: the effect of contact lens material and lens care solution. Invest. Ophthalmol. Vis. Sci. 51: 2843-2851.

Scherz W and Dohlman CH (1975). Is the lacrimal gland dispensable?: Keratoconjunctivitis sicca after lacrimal gland removal. Archives of Ophthalmology 93: 281-283.

Schlanger JL (1993). A study of contact lens failures. J. Am. Optom. Assoc. 64: 220-224.

Schuett BS and Millar TJ (2013). An investigation of the likely role of (O-acyl) omega-hydroxy fatty acids in meibomian lipid films using (O-oleyl) omega-hydroxy palmitic acid as a model. Exp. Eye Res. 115C: 57-64.

Setälä NL, Metso J, Jauhiainen M, Sajantila A, and Holopainen JM (2011). Dry eye symptoms are increased in mice deficient in phospholipid transfer protein (PLTP). Am. J. Pathol. 178: 2058-2065.

Smith JA, Albeitz J, Begley C, Caffery B, Nichols K, Schaumberg D, and Schein O (2007). The epidemiology of dry eye disease: report of the Epidemiology Subcommittee of the International Dry Eye WorkShop (2007). Ocul. Surf. 5: 93-107.

Spurr-Michaud S, Argueso P, and Gipson I (2007). Assay of mucins in human tear fluid. Exp. Eye Res. 84: 939-950.

Tei M, Spurr-Michaud SJ, Tisdale AS, and Gipson IK (2000). Vitamin A deficiency alters the expression of mucin genes by the rat ocular surface epithelium. Invest. Ophthalmol. Vis. Sci. 41: 82-88.

Tervo T, Joo F, Huikuri KT, Toth I, and Palkama A (1979). Fine structure of sensory nerves in the rat cornea: an experimental nerve degeneration study. Pain 6: 57-70.

Tiffany JM, (1997). Tears and conjunctiva. In: Harding JJ (Ed.). Biochemistry of the eye. Chapman & Hall, London, pp. 45-78

Torricelli AA, Singh V, Santhiago MR, and Wilson SE (2013). The Corneal Epithelial Basement Membrane: Structure, Function, and Disease. Invest. Ophthalmol. Vis. Sci. 54: 6390-6400.

Tsubota K and Nakamori K (1995). Effects of ocular surface area and blink rate on tear dynamics. Arch. Ophthalmol. 113: 155-158.

Uusitalo H, Chen E, Pfeiffer N, Brignole-Baudouin F, Kaarniranta K, Leino M, Puska P, Palmgren E, Hamacher T, Hofmann G, Petzold G, Richter U, Riedel T, Winter M, and Ropo A (2010). Switching from a preserved to a preservative-free prostaglandin preparation in topical glaucoma medication. Acta Ophthalmol. 88: 329-336.

Veldhuizen R, Nag K, Orgeig S, and Possmayer F (1998). The role of lipids in pulmonary surfactant. Biochim. Biophys. Acta 1408: 90-108.

Vonderahe AR (1928). Corneal and scleral anesthesia of the lower hale of the eye in a case of trauma of the superior maxillary nerve. Archives of Neurology & Psychiatry 20: 836-837.

Ward PP, Paz E, and Conneely OM (2005). Multifunctional roles of lactoferrin: a critical overview. Cell Mol. Life Sci. 62: 2540-2548.

Waring GO,3rd, Bourne WM, Edelhauser HF, and Kenyon KR (1982). The corneal endothelium. Normal and pathologic structure and function. Ophthalmology 89: 531-590.

Watanabe H (2002). Significance of mucin on the ocular surface. Cornea 21: S17-22.

Wattiez R, Hermans C, Cruyt C, Bernard A, and Falmagne P (2000). Human bronchoalveolar lavage fluid protein two-dimensional database: study of interstitial lung diseases. Electrophoresis 21: 2703-2712.

West-Mays JA and Dwivedi DJ (2006). The keratocyte: corneal stromal cell with variable repair phenotypes. Int. J. Biochem. Cell Biol. 38: 1625-1631.

Whikehart DR, (2004). Biochemistry of the eye. Butterworth-Heinemann, Boston, MA.

Wollensak G, Mur E, Mayr A, Baier G, Gottinger W, and Stoffler G (1990). Effective methods for the investigation of human tear film proteins and lipids. Graefes Arch. Clin. Exp. Ophthalmol. 228: 78-82.

Wong H, Fatt I, and Radke CJ (1996). Deposition and thinning of the human tear film. J. Colloid Interface Sci. 184: 44-51.

Yan W, Biswas SC, Laderas TG, and Hall SB (2007). The melting of pulmonary surfactant monolayers. J. Appl. Physiol. 102: 1739-1745.

Yeh PT, Casey R, and Glasgow BJ (2013). A novel fluorescent lipid probe for dry eye: retrieval by tear lipocalin in humans. Invest. Ophthalmol. Vis. Sci. 54: 1398-1410.

Yetukuri L, Katajamaa M, Medina-Gomez G, Seppänen-Laakso T, Vidal-Puig A, and Oresic M (2007). Bioinformatics strategies for lipidomics analysis: characterization of obesity related hepatic steatosis. BMC Syst. Biol. 1: 12.

Yokoi N, Yamada H, Mizukusa Y, Bron AJ, Tiffany JM, Kato T, and Kinoshita S (2008). Rheology of tear film lipid layer spread in normal and aqueous tear-deficient dry eyes. Invest. Ophthalmol. Vis. Sci. 49: 5319-5324.

Zander E and Weddel G (1951). Observations on the innervation of the cornea. J. Anat. 85: 68-99.

Zuo YY and Possmayer F (2007). How does pulmonary surfactant reduce surface tension to very low values? J. Appl. Physiol. 102: 1733-1734.

ORIGINAL PUBLICATIONS